Configuration Models for Moduli Spaces of Riemann Surfaces with Boundary

Carl-Friedrich Bödigheimer

Abstract

In this article we consider Riemann surfaces F of genus $g \geq 0$ with $n \geq 1$ incoming and $m \geq 1$ outgoing boundary circles, where on each incoming circle a point is marked. For the moduli space $\mathfrak{M}_g^\bullet(m,n)$ of all such F of genus $g \geq 0$ a configuration space model $\mathfrak{Rad}_h(m,n)$ is described : it consists of configurations of $h = 2g-2+m+n$ pairs of radial slits distributed over n annuli; certain combinatorial conditions must be satisfied to guarantee the genus g and exactly m outgoing circles. Our main result is a homeomorphism between $\mathfrak{Rad}_h(m,n)$ and $\mathfrak{M}_g^\bullet(m,n)$.

The space $\mathfrak{Rad}_h(m,n)$ is a non-compact manifold, and the complement of a subcomplex in a finite cell complex. This can be used for homological calculations. Furthermore, the family of spaces $\mathfrak{Rad}_h(m,n)$ form an operad, acting on various spaces connected to conformal field theories.

Contents

1 Introduction

1.1 Surfaces and their Moduli

This article explains a uniformization method of Riemann surfaces with boundary. The boundary must consist of a "incoming" and and "outgoing" curve; so the surface is a bordism between two non-empty compact 1-manifolds. We describe the moduli spaces of those surfaces by a kind of configuration space. A point in this space is a configuration of pairs of radial slits lying on disjoint annuli.
The Riemann surfaces F we consider have arbitrary genus $g \geq 0$, are connected and have two kinds of boundary curves, namely $n \geq 1$ incoming and $m \geq 1$ outgoing curves. The curves are numbered, and on each incoming curve a point is marked. The moduli space of such surfaces is denoted by $\mathfrak{M}_g^\bullet(m,n)$.

To this data F we will associate a configuration $\mathcal{L}$ consisting of $h = 2g - 2 + m + n$ pairs of radial slits in n fixed annuli in n disjoint complex planes. A slit is a radial cut from the outer boundary to some interior point. Slits which are paired must be of the same length, but may lie on different annuli. The number m is encoded in a combinatorial condition on the distribution and the interlocking of these slit pairs. The Figures [2 – 17] show plenty of examples.
Vice versa, given such a configuration L we can associate to it a surface $F = F(L)$ by identifying the right bank of a slit with the left bank of the slit paired with it. This surface is of the required topological type and has a canonical conformal structure.
The topology on the set $\mathfrak{Rad}_h(m,n)$ of all such configurations is such that the slits can move in the annuli, and when a shorter slit collides with a longer slit from the right (resp. left) bank, it can jump to the left (resp. right) bank of that slit to which the longer one is paired.

1.2 Results

In this way the (conformal equivalence classes of non-degenerate) surfaces F correspond precisely to the (equivalence classes of non-degenerate) configurations L. And this correspondence is a homeomorphism.

Theorem 1.1. *There is a homeomorphism*

$$\mathfrak{M}_g^\bullet(m,n) \longrightarrow \mathfrak{Rad}_h(m,n),$$

where $h = 2g - 2 + m + n$.

The n-dimensional torus group $\mathbb{T}^n = \mathbb{S}^1 \times \cdots \times \mathbb{S}^1$ acts on $\mathfrak{Rad}_h(m,n)$ by rotating the n annuli, and on $\mathfrak{M}_g^\bullet(m,n)$ by rotating the marked points along the incoming curves. The quotient of $\mathfrak{M}_g^\bullet(m,n)$ by this action is the (unmarked) moduli space $\mathfrak{M}_g(m,n)$.

1.3 Overview of the Sections

In **Section 2** we recall the necessary background on moduli spaces, Teichmüller spaces and mapping class groups of Riemann surfaces with boundary and marked points.

In **Section 3** we define and explain the notion of a radial slit domain, i.e., a configuration of h pairs of slits on n annuli satisfying certain combinatorial conditions. At this moment we will admit too many configurations, in other words do not yet exclude configurations leading to degenerate surfaces.

In **Section 4** we associate a surface $F(L)$ to any configuration. As already indicated, this surface is possibly degenerate; we will thus need to distinguish between degenerate and non-degenerate configurations. If $F(L)$ is non-degenerate, then it has a canonical conformal structure. Together with the numbering of the incoming and outgoing circles, the fixed marked points, its conformal class is a point in $\mathfrak{M}_g^\bullet(m,n)$ for $h = 2g-2+m+n$.

Section 5 is a continuation of Section 3, where we develop a reduced representation of a configuration L : it takes into account that in the non-generic case fewer than $2h$ slits may suffice. But this is conveniently described only after having the surfaces $F(L)$ seen built.

In **Section 6** we present the opposite direction, namely how to associate a configuration $L(F)$ to a surface F. This is called the Hilbert uniformization.

In **Section 7** we define the space $\mathrm{Rad}_h(m,n)$ of all configurations, and the open subspace $\mathfrak{Rad}_h(m,n)$ of non-degenerate configurations. We show that $\mathfrak{Rad}_h(m,n)$ is a manifold of dimension $6g-6+3m+4n$. Associating $L \mapsto F(L)$ and $F \mapsto L(F)$ as in Section 4 resp. Section 6 defines maps $\mathcal{G} : \mathfrak{Rad}_h(m,n) \to \mathfrak{M}_g^\bullet(m,n)$ and $\mathcal{H} : \mathfrak{M}_g^\bullet(m,n) \to \mathfrak{Rad}_h(m,n)$, where $h = 2g-2+m+n$. They are inverses of each other and they are homeomorphism. This proves the main result.

In **Section 8** we define a compactification $\mathrm{Rad}_h(m,n)$ as a cell complex. The degenerate surfaces added have not only pinched curves, but also handles degenerated to an interval. Thus this compactification is quite different from the Deligne-Mumford compactification. It can be used to compute the homology of $\mathfrak{M}_g^\bullet(m,n)$. See [ABE].

In **Section 9** we describe how to glue two surfaces F and F' when F' has as many incoming curves as F has outgoing curves. (Here we need to specify points not only on the incoming, but also on the outgoing curves; we denote the corresponing moduli spaces by $\mathfrak{M}_g^{\bullet\bullet}(m,n)$.) The gluing or composition) is a map $\mathfrak{M}_{g'}^{\bullet\bullet}(m',m)\times\mathfrak{M}_g^{\bullet\bullet}(m,n)\to\mathfrak{M}_{g'+g}^{\bullet\bullet}(m',n)$. In fact the family of spaces $\mathfrak{M}_g^{\bullet\bullet}(m,n)$ for all g,m,n form an operad (or more precisely, a properad).

For us one motivation to give this configuration-like description of moduli spaces lies in this advantages: to define this gluing of two "bordism surfaces" without refering to a parametrization of the boundary or to a collar of the boundary. This gluing is an important point in conformal field theories, and it is a notoriously difficult point.

The uniformization method we present here is named *Hilbert uniformization*, since it was used in [H] to represent single surfaces by parallel slit domains in the plane. In [B-1] we have described with this method a model for the moduli space of surfaces with only one boundary curve, namely parallel slit domains in the plane. It is similiar to the model presented here, but with less complicated combinatorics. See [B-2], [B-3] and [B-4] for further material. The model has been used in [E], [A] and [ABE] to compute the homology of the moduli space for $g=2$, $n=1$ and $m=0$. In [Z-1] a model for non-orientable surfaces was developed, and the homology for $g\leq 2$ was computed; see also [Z-2].

In a forthcoming article we will describe the space in a more combinatorial way.

Acknowledgements: The author would like to express his thanks to Johannes Ebert, Eva Mierendorff, Birgit Richter, Graeme Segal, and in particular to Ulrike Tillmann. He gratefully remembers the hospitality of Merton College, Oxford, during the summer term of 2002, while this material was worked out. Myint Zaw has been very helpful with the figures. We also thank the referee for useful suggestions.

2 The Moduli Spaces $\mathfrak{M}_g^{\bullet}(m,n)$

We will briefly recall some fundamental notions and results concerning moduli spaces of Riemann surfaces, Teichmüller spaces and mapping class groups. As a general reference see [Ab], [B], [GL].

2.1 Riemann Surfaces

The Riemann surfaces F we consider are connected, compact, with boundary and of arbitrary genus $g \geq 0$. The boundary ∂F is partitioned into two kinds of boundary curves, namely $n \geq 1$ incoming curves $C_1^-, \ldots, C_n^-$ and $m \geq 1$ outgoing curves $C_1^+, \ldots, C_m^+$. On each incoming curve we assume a point $P_r \in C_r^-$ to be chosen; we write $P = (P_1, \ldots, P_n)$, $C^- = C_1^- \cup \ldots \cup C_n^-$, $C^+ = C_1^+ \cup \ldots \cup C_m^+$. The partition into incoming and outgoing curves and their numbering, and the marked points are part of the structure.

Note that we do not have a parametrization of the boundary curves. This way we will avoid infinite-dimensional moduli spaces.

We can assume without loss of generality that for each boundary curve there exists a collar, i.e., it has a neighbourhood in F, which is conformally homeomorphic to a neighbourhood of $\mathbb{S}^1$ in the domain $\mathbb{D}^- = \{z| \ |z| \geq 1\}$ for incoming curves resp. in the domain $\mathbb{D}^+ = \{z| \ |z| \leq 1\}$ for outgoing curves. Therefore all holomorphic or harmonic maps and functions have an extension across the boundary.

Two such surfaces F and F' will be called *conformally equivalent*, if there is a conformal homeomorphism $h : F \to F'$ mapping a curve $C_i^{\pm}$ to $C_i'^{\pm}$. Thus h must preserve the type (in or out) and the number of the boundary curve. We call such a conformal equivalence *marked*, if P is mapped to P'. The equivalence classes are denoted by $[F]$ resp. $[F, P]$.
Note that these surfaces have no marked conformal automorphisms; and with the exception of annuli ($g = 0, n = m = 1$) they have also no unmarked conformal automorphisms.

2.2 Moduli Spaces

Let $\mathfrak{M}_g(m, n)$ resp. $\mathfrak{M}_g^\bullet(m, n)$ denote the set of all conformal resp. marked conformal equivalence classes of surfaces F as above.
The topology of these moduli spaces is given by the Teichmüller metric. To prepare its definition we call a subset $Q \subset F$ together with four specified points $q_1, \ldots, q_4$ on its boundary a *quadrilateral in* F if it is homeomophic to a closed rectangle in $\mathbb{C}$ such that the four corners correspond in counterclockwise orientation to $q_1, \ldots, q_4$. By the Riemann mapping theorem Q is even the conformal image of rectangle, i.e., there is a unique conformal mapping $\psi : Q \to R_{a,b} = [0, a] \times [0, b]$ such that $\psi(q_1) = (0, 0), \psi(q_2) = (a, 0), \psi(q_3) = (a, b), \psi(q_4) = (0, b)$. The ratio $\mathrm{mod}(Q) = b/a$ is called the *modulus* of Q.

Let $f : F \to F'$ be any homeomorphism between two surfaces. If Q is a quadrilateral in F, then $f(Q)$ is a quadrilateral in F'. The homeomorphism f is called *quasi-conformal*, if there is some real number $K \geq 1$ such that

$$\frac{1}{K} \operatorname{mod}(Q) \leq \operatorname{mod}(f(Q)) \leq K \operatorname{mod}(Q) \tag{2.1}$$

for all quadrilaterals Q in F. The infimum of all such K is denoted by $K[f]$ and is called the *maximal dilatation* of f. It suffices to consider quadrilaterals contained in a coordinate chart of the conformal atlas of F. Denote by $QC(F; F')$ the set of all quasi-conformal maps preserving the orientation, the partition and numbering of the boundary curves and denote by $QC(F, P; F', P')$ those preserving in addition the marked points.
The functional $K : f \mapsto K[f]$ on $QC(F, F')$ has the following properties :

$$K[f] = 1 \text{ if and only if } f \text{ is conformal.} \tag{2.2}$$

$$K[f] = K[f^{-1}] \tag{2.3}$$

$$K[f_1 \circ f_2] \leq K[f_1] \cdot K[f_2] \tag{2.4}$$

It follows that

$$\operatorname{dist}_{\mathfrak{M}}([F], [F']) = \frac{1}{2} \log \inf\{K[f] | f \in QC(F; F')\} \tag{2.5}$$

is a metric for $\mathfrak{M}_g(m, n)$. If we restrict f to be in $QC(F, P; F', P')$, then we obtain a metric $\operatorname{dist}_{\mathfrak{M}^\bullet}$ for $\mathfrak{M}_g^\bullet(m, n)$.

The forgetful map $\pi_{\mathfrak{M}} : \mathfrak{M}_g^\bullet(m, n) \to \mathfrak{M}_g(m, n)$, $[F, P] \mapsto [F]$ is obviously continuous; moreover, it is a $\mathbb{T}^n$-bundle, arising from a free action. An element $(t_1, \ldots, t_n)$ of the n-dimensional torus $\mathbb{T}^n = \mathbb{S}^1 \times \ldots \times \mathbb{S}^1$ acts on $\mathfrak{M}_g^\bullet(m, n)$ in the following way: if $P_i \in C_i^-$ corresponds under a conformal collar map to $p_i \in \mathbb{S}^1$, it is replaced by P_i' corresponding to $t_i\, p_i$. This is a well-defined action by isometries.

2.3 Teichmüller Spaces

To put this into the context of Teichmüller spaces we pick a fixed surface $\tilde{F}$ and consider all of its *conformal deformations*, i.e., quasi-conformal maps $\phi \in QC(\tilde{F}; F)$ for some F.
Two such deformations are called *(conformally) equivalent*, if there is some conformal $f : F \to F'$, which is homotopic to $\phi^{-1} \circ \phi'$, where the homotopy is constant on the boundary. The set of marked deformation classes with the metric

$$\operatorname{dist}_{\mathfrak{T}}([\phi], [\phi']) = \frac{1}{2} \log \inf\{K[f] | f \in QC(F; F'),\ f \simeq \phi^{-1} \circ \phi'\} \tag{2.6}$$

is the *Teichmüller space* $\mathfrak{T}_g(m,n)$. The set of marked deformation classes, with the corresponding metric $\mathrm{dist}_{\mathfrak{T}^\bullet}$ as above, is the marked Teichmüller space $\mathfrak{T}_g^\bullet(m,n)$. Its elements are denoted by $[\phi, P]$.

There is an analogous forgetful map $\pi_{\mathfrak{T}} : \mathfrak{T}_g^\bullet(m,n) \to \mathfrak{T}_g(m,n)$ between Teichmüller spaces. It is a trivial fibre bundle, i.e., $\mathfrak{T}_g^\bullet(m,n) \simeq \mathfrak{T}_g(m,n) \times \mathbb{T}^n$. The maps $\tau^\bullet : \mathfrak{T}_g^\bullet(m,n) \to \mathfrak{M}_g^\bullet(m,n)$ given by $[\phi, P] \mapsto [F, P]$ resp. $[\phi] \mapsto [F]$ are obviously both continuous and surjective.

2.4 Mapping Class Groups

The maps $\tau^\bullet$ and τ are invariant under the action of the *mapping class group* $\Gamma_g(m,n) = \pi_0(\mathrm{Diff}^+(F, \partial F))$ of isotopy classes of orientation-preserving diffeomorphisms which fix the boundary pointwise. (There is no difference between $\Gamma_g^\bullet(m,n)$, $\Gamma_g(m,n)$ and $\Gamma_{g,m+n}$, the latter being the mapping class group with $m+n$ boundary curves, not partitioned into incoming and outgoing ones.) The action of $\gamma \in \Gamma_g(m,n)$ on $\mathfrak{T}_g^\bullet(m,n)$ is given by $[\phi, P].[\gamma] = [\phi \circ \gamma, P]$ and on $\mathfrak{T}_g(m,n)$ by $[\phi].[\gamma] = [\phi \circ \gamma]$. Note that diffeomorphisms are quasi-conformal. The action is by isometries with respect to the Teichmüller metric, and thus properly-discontinuously. It is also free — except in the case of an annulus ($g = 0, m = n = 1$) : its isotropy groups at the point $[\phi] \in \mathfrak{T}_g(m,n)$ are the automorphisms of $[F]$, and they are all trivial. Thus $\mathfrak{M}_g(m,n) = \mathfrak{T}_g(m,n)/\Gamma_g(m,n)$, and $\mathfrak{T}_g(m,n)$ is an unbranched covering space of $\mathfrak{M}_g(m,n)$. Using the fact that the Teichmüller space $\mathfrak{T}_g(m,n)$ is homeomorphic to an open ball of dimension $6g - 6 + 3m + 3n$, it follows that the moduli space $\mathfrak{M}_g(m,n)$ is a (topological) manifold, and furthermore, that $\mathfrak{M}_g(m,n)$ is a classifying space $B\Gamma_g(m,n)$ for the mapping class group $\Gamma_g(m,n)$.

We have the following commutative square :

(2.7)
$$\begin{array}{ccccc}
\Gamma_g(m,n) & = & \Gamma_g^\bullet(m,n) & = & \Gamma_{g,m+n} \\
\downarrow & & \downarrow & & \\
\mathfrak{T}_g(m,n) & \xleftarrow{\pi_{\mathfrak{T}}} & \mathfrak{T}_g^\bullet(m,n) & \xleftarrow{\cong} & \mathfrak{T}_g(m,n) \times \mathbb{T}^n \\
\tau \downarrow & & \downarrow \tau^\bullet & & \\
\mathfrak{M}_g(m,n) & \xleftarrow{\pi_{\mathfrak{M}}} & \mathfrak{M}_g^\bullet(m,n) & &
\end{array}$$

The mapping class group $\Gamma_g(m,n)$ is a torsion-free central extension of the mapping class group $\Gamma_g^{m,n}$ of a closed surface of genus g with $m+n$ marked

points :

$$1 \to \mathbb{Z}^{m+n} \to \Gamma_g(m,n) \to \Gamma_g^{m+n} \to 1 \tag{2.8}$$

The kernel of this extension is generated by Dehn-twists around the boundary circles. The group Γ_g^{m+n} in turn is an extension of the mapping class group Γ_g of a closed surface

$$1 \to \pi_1(\tilde{C}^{m+n}(F)) \to \Gamma_g^{m+n} \to \Gamma_g \to 1 \tag{2.9}$$

where $\tilde{C}^{m+n}(F)$ is the ordered configuration space of $m+n$ points in F.

3 Radial Slit Configurations

3.1 Slit Annuli

Let $\mathbb{A} = \{z \in \mathbb{C} \mid R_1 \leq |z| \leq R_0\}$ denote a closed annulus in the complex plane, with inner and outer radii $0 < R_1 < R_0$. We fix n such annuli $\mathbb{A}_1, \ldots, \mathbb{A}_n$ on n distinct complex planes; their outer radii are all equal to R_0, but their inner radii $R_1, \ldots, R_n$ may be distinct. Their disjoint union is denoted by $\mathbb{B} = \mathbb{A}_1 \sqcup \cdots \sqcup \mathbb{A}_n$.

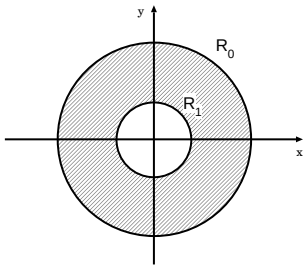

Figure 1: *Annulus in complex plane.*

Set

$$h = 2g - 2 + m + n \tag{3.1}$$

and consider $2h$ points $\zeta_1, \ldots, \zeta_{2h}$ in $\mathbb{B}$, which we call *(slit) endpoints*. The set $I := \underline{2h} = \{1, \ldots, 2h\}$ will be called *index set*. We consider the sequence $\zeta = (\zeta_1, \ldots, \zeta_{2h})$ sometimes as a function $\zeta : I \to \mathbb{B}$, $\zeta(k) = \zeta_k$. The

distribution function $\nu : I \to \underline{n} = \{1, \ldots, n\}$ is given by $\zeta_k \in \mathbb{A}_{\nu(k)}$. We assume that there is at least one endpoint on each annulus, thus

$$I_r := \nu^{-1}(r) \neq \emptyset, \text{ for all } r \in \underline{n}, \tag{3.2}$$

which we call *partial index set for the annulus* $\mathbb{A}_r$. Let $\theta : I \to \mathbb{S}^1$ be the *argument function* $\theta(k) = \arg(\zeta_k)$. The sets

$$S_k = \{z \in \mathbb{A}_{\nu(k)} | \arg(z) = \theta(k), |z| \geq |\zeta_k|\} \tag{3.3}$$

$$S'_k = \{z \in \mathbb{A}_{\nu(k)} | \arg(z) = \theta(k)\} \tag{3.4}$$

are called the *slit* resp. the *radial segment starting at* ζ_k. If the arguments $\theta(i)$ and $\theta(j)$ for any two i, j in the same I_r are distinct, i.e., the S'_k are disjoint, we call this the *generic case*.

The numbering of the endpoints ζ_k will turn out to be arbitrary. But if two endpoints ζ_i and ζ_j on the same annulus $\mathbb{A}_r$ have the same argument or if they coincide, it is necessary to know a cyclic ordering of the endpoints on each annulus. Therefore we need a *cyclic successor permutation* ω in the symmetric group $\mathfrak{S}_{2h} = \mathfrak{S}(I)$ of I satisfying

$$I_1, \ldots, I_n \text{ are the cycles of } \omega. \tag{3.5}$$

$$\theta \text{ is weakly monotonic on each } I_1, \ldots I_n. \tag{3.6}$$

In the generic case ω is, of course, determined by the position of the endpoints. In the non–generic case however, ω contains essential information about the topology of the surface to be associated to the configuration and about the topology of the space of all configurations.

Let us write $\theta(k) = \arg(\zeta_k)$ as $\exp(2\pi\sqrt{-1}\, t'_k)$ for $0 \leq t'_k \leq 1$. If $I_r = \langle k, \omega(k), \omega^2(k), \ldots \rangle$, then $0 \leq t'_k \leq t'_{\omega(k)} \leq \ldots \leq 1$. We set $t_k = t'_{\omega(k)} - t'_k$ and have $\sum_{i \in I_r} t_i = 1$. (Later we shall use these t_i as barycentric coordinates of our configuration.)

The function ν is ω-invariant; it will serve as a numbering of the the incoming boundary curves.

There are two cases which need special consideration.

(a) Firstly, $\omega(k) = k$, i.e., $I_{\nu(k)} = \langle k \rangle$ for some $k \in I$, means there is only the endpoint ζ_k on $\mathbb{A}_{\nu(k)}$.

(b) Secondly, $\omega(k) = l$, $\omega(l) = k$ and $\theta(k) = \theta(l)$, i.e., $I_{\nu(k)} = \langle k, l \rangle$ for some $k, l \in I$, means there are only the two endpoints ζ_k, ζ_l on $\mathbb{A}_{\nu(k)}$.

In these two cases there is an ambiguity : t_k resp. t_k or t_l can be put 0 or 1.

We see case (b) as a limit of a generic configuration, but we need to distinguish, whether say ζ_l approached S'_k from the right or from the left. And in case (b) this can not be extracted from ω alone. To dissolve this ambiguity we put those *exceptional indices* into a subset $\Xi \subset I$ with the property :

$$\text{If } k \in \Xi, \text{ then } \theta(\omega(k)) = \theta(k), \text{ i.e., } t_k = 0. \tag{3.7}$$

$$\text{If } k \neq \omega(k) \text{ and } \theta(\omega(k)) = \theta(k), \text{ then} \tag{3.8}$$
$$\text{either } k \in \Xi \text{ or } \omega(k) \in \Xi, \text{ i.e., either } t_k = 0 \text{ or } t_{\omega(k)} = 0.$$

Note that the case (b) $I_r = \langle k, \omega(k) \rangle$ is the only case where $k \in \Xi$ or $k \notin \Xi$ are both possible, but need to be distinguished : $k \in \Xi$ means the slit $S_{\omega(k)}$ touches the radial segment S'_k from the left; and $\omega(k) \in \Xi$ means the slit $S_{\omega(k)}$ touches the radial segment S'_k from the right. Obviously, $\Xi = \emptyset$ only in the generic case.

The points ζ_k need to be *paired* by a fix-point-free involution $\lambda \in \mathfrak{S}_{2h}$, i.e.,

$$\lambda^2(k) = k \text{ and } \lambda(k) \neq k \text{ for all } k \in I. \tag{3.9}$$

Paired endpoints must satisfy

$$|\zeta_k| = |\zeta_{\lambda(k)}| \text{ for all } k \in I. \tag{3.10}$$

They can lie on the same or on different annuli; but the pairs must connect all n annuli in the following sense. Regard $\underline{n}$ as the vertex set of a graph G, with an edge between two vertices r_1 and r_2 if and only if there is some $k \in I$ with $\nu(k) = r_1$ and $\nu(\lambda(k)) = r_2$ (i.e., one endpoint of the pair k, $\lambda(k)$ lies on $\mathbb{A}_{r_1}$ and the other on $\mathbb{A}_{r_2}$). We demand that

$$G \text{ is connected .} \tag{3.11}$$

In other words, the subgroup of $\mathfrak{S}_{2h}$ generated by λ and ω acts transitively on the set I. It follows that $n - 1 \leq h$.
The *exchange permutation* defined by $\kappa = \lambda \circ \omega \in \mathfrak{S}_{2h}$ will determine the number of outgoing boundary circles of the surface. The condition on κ is :

$$\kappa \text{ has } m \text{ cycles .} \tag{3.12}$$

As a last piece of information we need a κ-invariant *redistribution function* $\mu : I \to \underline{m}$, i.e.,

$$\mu(\kappa(k)) = \mu(k) \text{ for all } k \in I. \tag{3.13}$$

It corresponds to the ω-invariant function $\nu : I \to \underline{n}$, and will serve as a numbering of the outgoing boundary curves..

To summarize, the data necessary to describe a configuration is :
– the outer radius and the inner radii $R = (R_0, R_1, \ldots, R_n)$
– the $2h$ endpoints $\zeta = (\zeta_1, \ldots, \zeta_{2h})$ in $\mathbb{B}$
– the pairing $\lambda \in \mathfrak{S}_{2h}$,
– the successor permutation $\omega \in \mathfrak{S}_{2h}$,
– the set $\Xi \subset I$ of exceptional indices,
– the redistribution function $\mu : I \to \underline{m}$
such that the conditions (3.1) to (3.13) are satisfied. The index set I is fixed. The function ν, the function θ and the permutation κ are derived from this data and do not involve any choices. We call

$$L = (\zeta; \lambda, \omega, \mu, \Xi; R) = (\zeta_1, \ldots, \zeta_{2h}; \lambda, \omega, \mu, \Xi, ; R_0, R_1, \ldots, R_n) \tag{3.14}$$

a *radial slit configuration of h slit pairs on n annuli with outer radius R_0 and inner radii $R_1, \ldots, R_n$.*

So far we have not made any restrictions about the position of the endpoints; they are allowed to have equal arguments, to even coincide and to lie an the boundary of the annuli. We will see in section 4, where we associate a surface with a configuration, that some, but not all of this may be allowed.

3.2 Examples of Configurations

We will show some figures with configurations and indicated the surface, – obtained by identifying the right bank of the slit S_k with the left bank of $S_{\lambda(k)}$. To keep the notation easy, we enumerate the endpoints counterclockwise on each annulus. The annuli are numbered from left to right. Some data (like radii) will not be specified.

The easiest configuration possible is the *empty* configuration on one annulus as shown in Figure [2].
The configuration of Figure [3] with $n = h = 1$ is the easiest non-empty configuration. The pairing λ is $\langle 1, 2\rangle$, and ω is also $\langle 1, 2\rangle$. Thus $\kappa = \langle 1\rangle\langle 2\rangle$, which implies $m = 2$, and thus $g = 0$. The numbering of the κ-cycles is not specified, and similarily the radii R_0 and R_1. As in all generic cases Ξ is empty.
In Figure [4] we have one pair of slits on two annuli with different (and unspecified) inner radii R_1, R_2. The pairing λ is obvious, and there is only

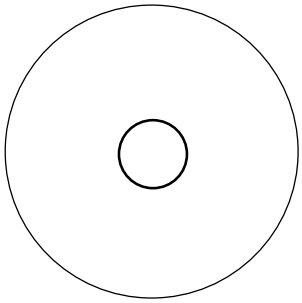

Figure 2: *An empty annulus : n=1, h=0, m=1 and g=0.*

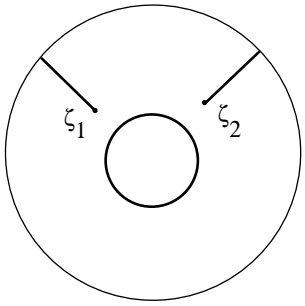

Figure 3: *n=1, h=1, m=2, g=0 : a pair-of-pants with one incoming and two outgoing boundary circles.*

one κ-cycle. With $n = 2$, $h = 1$ and $m = 1$ we find $g = 0$. Like Figure [3] it is a pair-of-pants, but with the role of the incoming and outgoing boundary circles exchanged; furthermore, the two incoming tubes have different length.

In Figure [5] we see two pairs of slits on two annuli of different inner radii, three slits on the first annulus and one on the second. Since κ has the two cycles $\langle 1, 4, 2\rangle$ and $\langle 3\rangle$, we have $m = 2$ and therefore $g = 0$. Thus it is a planar surface with 4 boundary curves, where the numbering of the two outgoing curves is not specified.
The easiest non-planar surface will be associated to a configuration as in Figure [6]. We have $n = 1$, and $h = 2$; the pairing is $\lambda = \langle 1, 3\rangle\langle 2, 4\rangle$, and thus $\kappa = \langle 1, 4, 3, 2\rangle$, and $m = 1$. The pair ζ_1, ζ_3 alone produces a pair-of-pants. Then the second pair ζ_2, ζ_4 represents a slit on each leg and leads therefore to a handle (with one incoming and one outgoing boundary circle.)

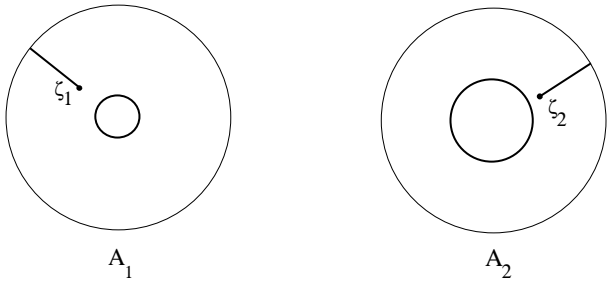

Figure 4: $n = 2, h = 1, m = 1, g = 0$ *: a pair-of-pants with two incoming and one outgoing boundary circles.*

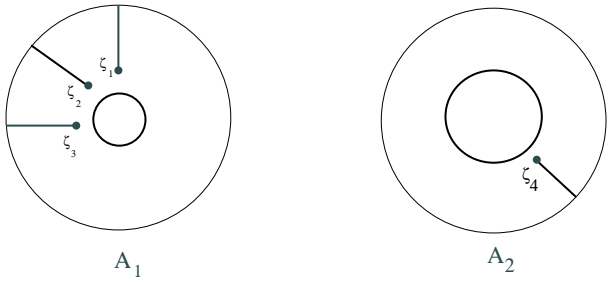

Figure 5: $n = 2, h = 2, m = 2, g = 0$ *with the pairing* $\lambda = \langle 1, 3\rangle\langle 2, 4\rangle$

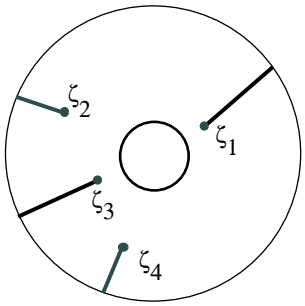

Figure 6: *A generic configuration with* $n = 1, h = 2, m = 1, g = 1$.

We repeat this configuration in Figure [7] (left picture), and contrast it

with the right picture : there on the right we also have $n = 1$ and $h = 2$, but the pairing is $\lambda = \langle 1,4\rangle\langle 2,3\rangle$, and thus with $\omega = \langle 1,2,3,4\rangle$ we find $\kappa = \langle 1,3\rangle\langle 2\rangle\langle 4\rangle$ and thus $m = 3$ and $g = 0$. The numbering μ is not specified. First the pair ζ_1, ζ_4 produces a pair-of-pants. But since the pair ζ_2, ζ_3 represent two slits on one and the same leg, we obtain altogether three legs, i.e., a planar surface with one incoming and three outgoing boundary curves.

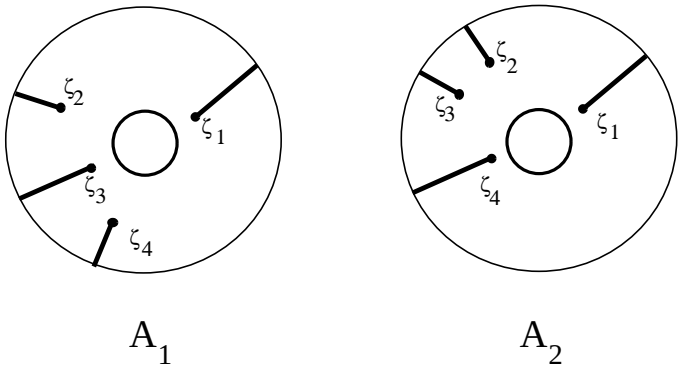

Figure 7: *Two configurations with $n = 1, h = 2$. In the left picture the pairs are interlocking and therefore $m = 1, g = 1$. In the right example the pairs are not interlocking and therefore $m = 3, g = 0$.*

The easiest non–generic configuration is shown in Figure [8]. It represents a degenerate surface, as we will see in detail in section 4. Here $\zeta_1 = \zeta_2$ and $\Xi = \{1\}$. The pairing λ is obvious. And $\kappa = \langle 1\rangle\langle 2\rangle$ has two cycles. Thus $h = 1, n = 1, m = 2$ and $g = 0$. One leg of the expected pair-of-pants is pinched along its entire length, i.e., has vanishing circumference.
The two different configurations of Figure [9] are non-generic, but represent non-degenerate surfaces, which are moreover of the same topological type. Indeed, their topological type is the same as the surface associated to Figure [6]. In the left picture ζ_2 was moved counterclockwise and touches the slit S_3 from the right and in the right picture it was moved clockwise and touches S_1 from the left. We shall see that both configurations represent the same i.e., conformally equivalent, surfaces. Going from the left configuration to the right one will be called a *jump*. The movement indicated is a Dehn twist.

If in Figure [9], left picture, the modulus of ζ_2 and ζ_4 are made the same as $|\zeta_1| = |\zeta_3|$, we obtain the configuration shown in Figure [10]. Its surface

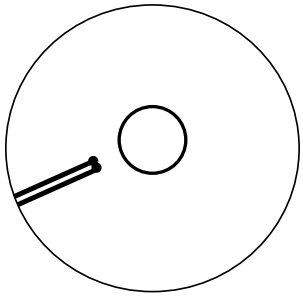

Figure 8: *A degenerate configuration, leading to a pinched tube.*

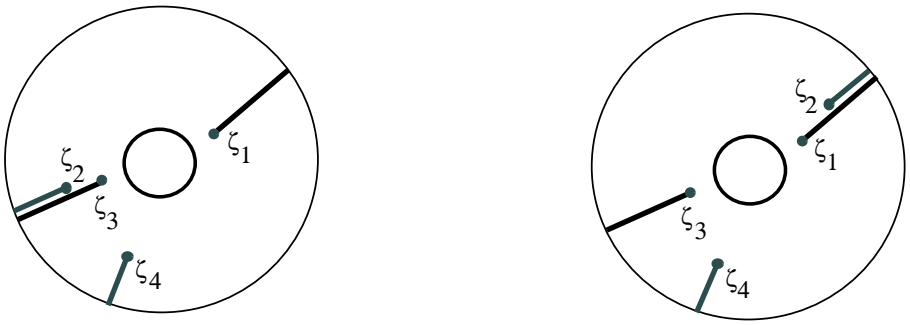

Figure 9: *A jump : the slit S_2 jumps from the right bank of S_3 to the left bank of S_1.*

is non-generic and non-degenerate, and again of the same topological, but different conformal type as [9].
If in Figure [9], left picture, ζ_4 is moved towards S_3, such that ζ_2 and ζ_4 actually agree, but touch S_3 from different sides, we obtain the configuration in Figure [11]. It is not generic and not degenerate, and of the same topological, but different conformal type as [6].
If in Figure [11] the modulus of ζ_3 (and thus of ζ_1 as well) is made equal or greater than the modulus of ζ_2 and ζ_4, then we obtain in Figure [12] a configuration, which represents a degenerate surface. What was a handle before degenerated into an interval.
In Figures [13] and [14] we show two symmetric configurations. A symmetry does not mean an automorphism of the associated surface as a marked conformal class in $\mathfrak{M}_1^\bullet(1,1)$, since we need to fix the marked points. But

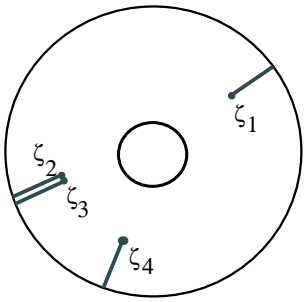

Figure 10: *A non-generic, but non-degenerate configuration with* $n = 1$, $h = 2$, $m = 1$ *and* $g = 1$.

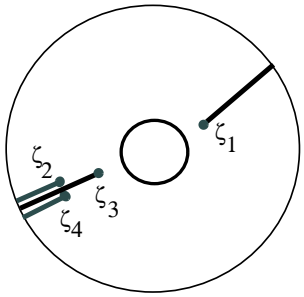

Figure 11: *A non-generic, but non-degenerate configuration with* $n = 1$, $h = 2$, $m = 1$ *and* $g = 1$.

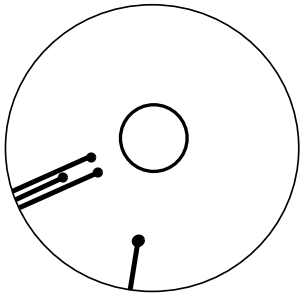

Figure 12: *A degenerate configuration, leading to a pinched handle.*

for the unmarked conformal class, i.e., in the moduli space $\mathfrak{M}_1(1,1)$, they

represent surfaces with automorphisms.

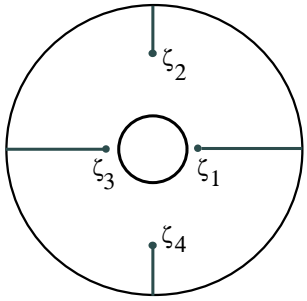

Figure 13: $n = 1, h = 2, m = 1, g = 1$ *: A configuration with a* $\mathbb{Z}/2$*-symmetry.*

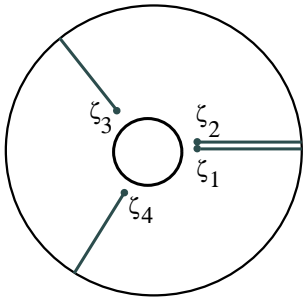

Figure 14: 14 $n = 1, h = 2, m = 1, g = 1$ *: A configuration with a* $\mathbb{Z}/3$*-symmetry.*

The configuration in Figure [15] is a typical case of genus $g = 2$ with two incoming and two outgoing boundary circles. Thus we need six pairs of slits on two annuli, chosen with different inner radii. As an example, we give here the full notation : $R_0 = 1.0, R_1 = 0.2, R_2 = 0.6$ are the common outer and the two inner radii for the annulus $\mathbb{A}_1$ on the left and $\mathbb{A}_2$ on the right, $I = \{1, \ldots, 12\}$ is the index set, $\lambda = \langle 1, 6\rangle\langle 2, 9\rangle\langle 3, 7\rangle\langle 4, 11\rangle\langle 5, 12\rangle\langle 8, 10\rangle$ is the pairing, the endpoints $\zeta = (\zeta_1, \ldots, \zeta_{12})$ are as shown in the figure, $\omega = \langle 1, 2, 3, 4, 5, 6, 7, 8, 9, 10\rangle\langle 11, 12\rangle$, and $\Xi = \{4, 8, 9\}$ are the three exceptional indices. The distribution function ν is 1 for the indices $1, \ldots 10$ and 2 for the indices $11, 12$. The exchange permutation κ has the cycles $\langle 1, 9, 8, 2, 7, 10, 6, 3, 11, 5\rangle$ and $\langle 4, 12\rangle$. The outer boundary parts are num-

bered according to the slit at which they start; notice that for the three exceptional indices 4, 8 and 9 those parts are only points.

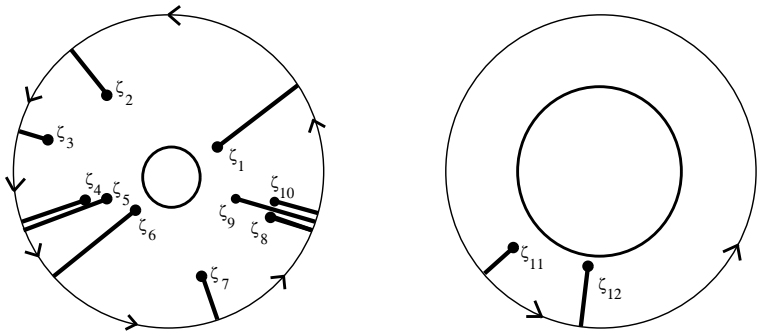

Figure 15: *A configuration with* $n = 2, h = 6, m = 2, g = 2$. *The pairing* λ *is* $\langle 1,6\rangle\langle 2,9\rangle\langle 3,7\rangle\langle 4,11\rangle\langle 5,12\rangle\langle 8,10\rangle$. *There are three exceptional indices* $4, 8$ *and* 9. *The two outgoing circles consist of the pieces* $\langle 1,9,8,2,7,10,6,3,11,5\rangle$ *and* $\langle 4,12\rangle$.

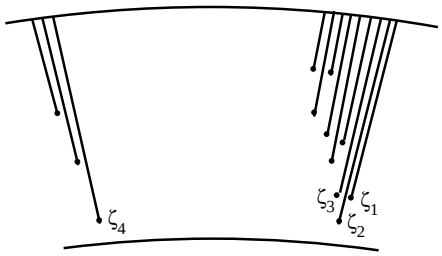

Figure 16: *A configuration concentrated on two radial segments.*

We end this gallery with two extreme examples. In Figure [16] we show an example of a configuration where all slits lie on only two radial segments of one annulus, but with different moduli. There are subconfigurations of two pairs like in Figure [11]. Obviously, the number g of such groups can be arbitrary; in our example $g = 3$. The surface $F(L)$ is non-degenerate of genus g and $n = m = 1$.
In Figure [17] we show another extreme case : $h = 2g$ of the $4g$ endpoints coincide; they are paired to $2g$ disjoint slits. There are subconfigurations of two pairs like in Figure [14]. The surface is of the same topological type as in Figure [16], namely $g = 3$, and $n = m = 1$.

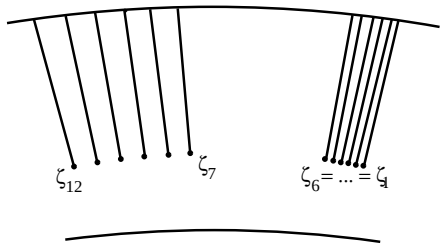

Figure 17: *A configuration with all slits of the same length and half of the endpoints coinciding.*

Later we will refer to several of these figures when we construct the surface associated to a configuration.

4 The Surface Associated to a Configuration

We need to associate a surface $F(L)$ to a configuration L, given in non-reduced notation. The basic idea is quite simple : for each slit S_k induced by its endpoint $\zeta_k \in \mathbb{A}_r$ we consider its complement $\mathbb{A}_r - S_k$ in $\mathbb{A}_r$ and add ideal boundary points, forming a right and left bank of S_k. These banks will be identified pairwise, namely the right bank of S_k with the left bank of $S_{\lambda(k)}$ and the left bank of S_k with the right bank of $S_{\lambda(k)}$.
For a generic configuration this procedure will lead to a topological surface with an obvious complex structure. But in the non-generic case we need to apply some care.

4.1 Radial Sectors

We dissect $\mathbb{B}$ (or rather the various annuli) along the radial segments S'_k, add a left and right ideal boundary edge and obtoin $2h$ sectors F_k. Choose $k \in I$ and set $l = \omega(k)$; then ζ_k and ζ_l are on the same annulus $\mathbb{A}_r$, where $r = \nu(k)$. We distinguish four cases :

(Case I) $k \neq l$ **and** $\theta(k) \neq \theta(l)$ **:**
We define $F_k = \{z \in \mathbb{A}_r \mid \theta(k) \leq \arg(z) \leq \theta(l)\}$, i.e., it is the closed sector of $\mathbb{A}_r$ between the radial segments S'_k and S'_l. See the left picture in Figure [18].

(Case II) $k \neq l$**, but** $\arg(\zeta_k) = \arg(\zeta_l)$ **and** $k \in \Theta$ **:**
We define F_k to be the radial segment S'_k. We call such a sector *thin*, and

Figure 18: *A proper sector (left picture) in Case I, and a thin sector (right picture) in Case II.*

all other sectors *proper*. See the right picture in Figure [18].

(Case III) $k \neq l$**, but** $\theta(k) = \theta(l)$ **and** $l \in \Xi$ **:**
We define F_k to be $\mathbb{A}_r$ cut open along S'_k and two ideal boundary edges added. Thus F_k is the annulus $\mathbb{A}_r$, but with radial segment doubled. Note that here $\omega(l) = k$, i.e., $I_r = \langle k, l \rangle$ and F_l is a thin sector and falls under Case II. See the left picture in Figure [19].

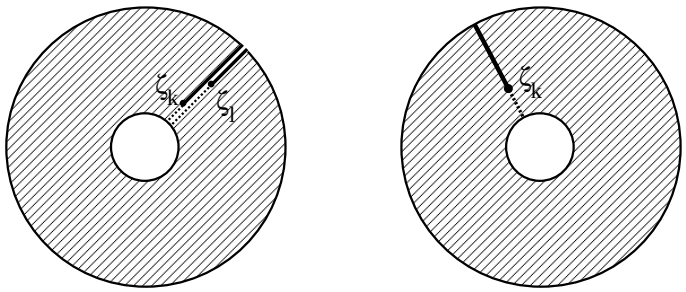

Figure 19: *The sectors in Case III (left picture) and Case IV (right picture) cover an entire annulus.*

(Case IV) $k = l$ **:**
Like in Case III we define F_k to be an annulus cut open along S'_k and with two ideal boundary edges added. Note that now $I_r = \langle k \rangle$, i.e., ζ_k is the only endpoint on $\mathbb{A}_r$. See the right picture of Figure [19].

Looking outward each sector F_k has a right edge E_k^- and a left edge E_k^+, called *ideal boundary edges*; see Figure [20]. In case II we have $F_k = E_k^- = E_k^+$; see Figure [21]. But in all other cases the two edges are (or are to

be regarded as) distinct. Since we regard all sectors as disjoint, we denote a point of F_k simply by z if it is not in the ideal boundary; but a point $z = \xi \exp(2\pi\sqrt{-1}\, t_k)$ in the boundary edge E_k^- is denoted by $(\xi, k, -)$ resp. in E_k^+ by $(\xi, k, +)$, where $R_{\nu(k)} \leq \xi \leq R_0$. The endpoint ζ_k occurs as $(|\zeta_k|, k, -)$ in F_k on the right ideal boundary E_k^-, and as $(|\zeta_k|, \omega^{-1}(k), +)$ on the left ideal boundary $E_{\omega^{-1}(k)}^+$ of the preceding sector $F_{\omega^{-1}(k)}$. See Figures [20] and [21].

We will regard a sector F_k as *lying over* $\mathbb{A}_{\nu(k)}$. The image of F_k intersects the images of $F_{\omega(k)}$ and of $F_{\omega^{-1}(k)}$. All F_k with $k \in I_r$ cover the annulus $\mathbb{A}_r$. We can use ω to give the set of all sectors lying over $\mathbb{A}_r$ a cyclic ordering.

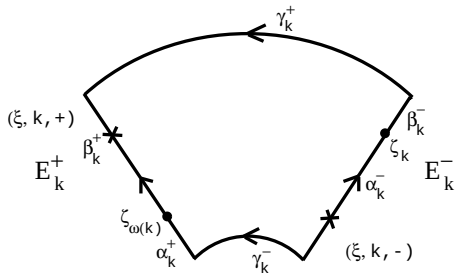

Figure 20: *The ideal boundary edges of a proper sector.*

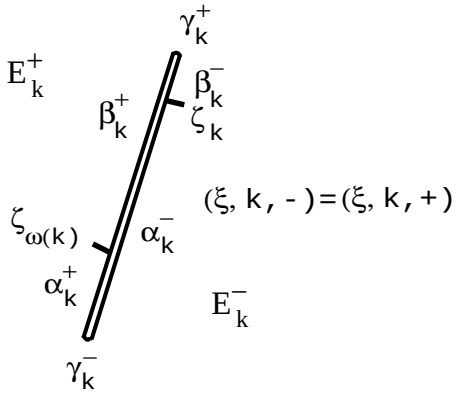

Figure 21: *The ideal boundary edges of a thin sector.*

Each sector F_k has an outer boundary curve denoted γ_k^+ and an inner boundary curve γ_k^-; for an exceptional $k \in \Xi$ both curves are only points. It will

be convenient to denote by α_k^- the part of E_k^- from the inner curve to ζ_k, by β_k^- the part of E_k^- from ζ_k to the outer curve, by α_k^+ the part of E_k^+ from the inner curve to $\zeta_{\omega(k)}$, by β_k^+ the part of E_k^+ from $\zeta_{\omega(k)}$ to the outer curve. See Figures [20] and [21].

4.2 Gluing

On the space $\bar{F}(L) = \bigsqcup_{k=1}^{2h} F_k$ we make the following boundary identifications. For $k \in I$ and z in the ideal boundary of F_k declare

$$(\xi, k, +) \approx (\xi, \omega(k), -), \quad \text{if } \xi \leq |\zeta_{\omega(k)}| \tag{4.1}$$

$$(\xi, k, +) \approx (\xi, \kappa(k), -), \quad \text{if } \xi \geq |\zeta_{\kappa(k)}| \tag{4.2}$$

$$(\xi, k, -) \approx (\xi, \omega^{-1}(k), +), \quad \text{if } \xi \leq |\zeta_k| \tag{4.3}$$

$$(\xi, k, -) \approx (\xi, \kappa^{-1}(k), +), \quad \text{if } \xi \geq |\zeta_k| \tag{4.4}$$

We define

$$F(L) := \bar{F}(L)/\approx \tag{4.5}$$

and call it the *associated surface*, although the surface is possibly degenerate.

In other words, the equivalence relation identifies α_l^- with $\alpha_{\omega^{-1}(l)}^+$ and β_l^- with $\beta_{\kappa^{-1}(l)}^+$. The identifications of two α-curves are within the same annulus, but the two identified β-curves are possibly on two different annuli. (Note that the last two lines of the declaration are redundant and not needed to generate the equivalence relation.) Let $q_L : \bar{F}(L) \to F(L)$ denote the quotient map. The image of all curves γ_k^+ resp. γ_k^- we call the *outgoing* resp. *incoming boundary* $\partial^+(F(L))$ resp. $\partial^-(F(L))$.

There are four questions arising :

4.2(a) Is $F(L)$ always a non-degenerate (topological) surface ?
4.2(b) Is there an obvious complex structure on $F(L)$?
4.2(c) Is any Riemann surface F representable as $F(L)$ for some L ?
4.2(d) Can $F(L_1)$, $F(L_2)$ be conformally equivalent for different L_1, L_2 ?

In this section we address questions 4.2(a) and 4.2(b); questions 4.2(c) and 4.2(d) will be answered in sections 6 and 7, respectively.

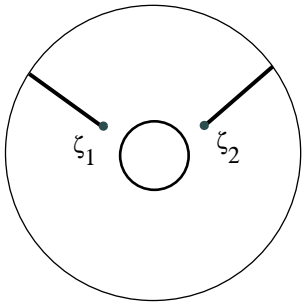

Figure 22: *The configuration* L *:* $n = 1, h = 1, m = 2, g = 0$.

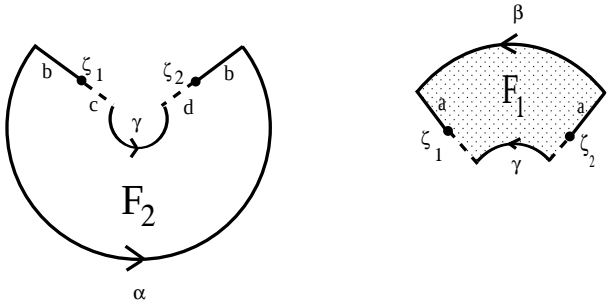

Figure 23: *The two sectors* F_1, F_2.

4.3 Examples of Surfaces

We show this gluing procedure step-by-step in two examples.
The easiest configuration possible, the case $n = 1$, $h = 1$, $m = 2$, $g = 0$, , is shown in Figure [22]: L is generic and has only one pair of slits on one annulus.
We perform cuts along the rays S_1' and S_2' and attach the ideal boundary edges to both sectors F_1 and F_2. See Figure [23].
The Figure [24] shows the finished surface in three-space.

A second example is shown in Figure [25]. The first picture shows a generic configuration L with $n = 1$, $h = 2$, $m = 1$ and thus $g = 1$, a torus with one incoming and one outgoing boundary circle. The middle picture shows an intermediate stage of the cut-and-paste process in three-space. The last picture is the finished surface $F(L)$. The labels $a, \ldots, d$ occur always twice, at the two edges to be identified.

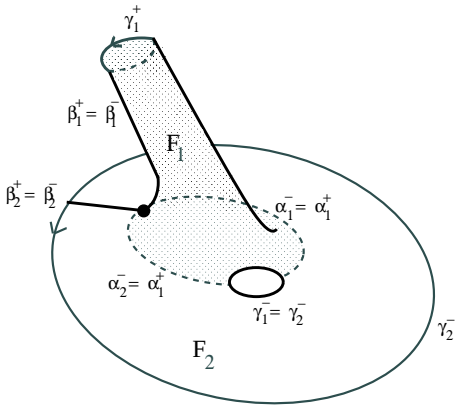

Figure 24: *The two sectors F_1, F_2 glued together.*

4.4 Degenerate Configurations

The question 4.2(a) has a negative answer, as can be seen from the example in Figure [26] : assume there is in a configuration L a pair $l = \lambda(k)$ with coinciding endpoints $\zeta_k = \zeta_l$ following each other in the cyclic order on some annulus, i.e., $l = \omega(k)$; then the gluing process attaches $\alpha_k^- = \alpha_k^+$ to the neighbouring sectors to the right and to the left, but $\beta_k^- = \beta_k^+$ are identitied only with each other. In other words we have an interval attached to the surface at one end. Compare this to Figure [24]: there the proper sector F_1 formed a proper tube with non-trivial longitude and meridian. Here in Figure [26] all meridians degenerated into points, making the circumference (and the corresponding homotopy or homology class) vanish.

The configuration of Figure [27] is of a similiar nature : the two endpoints $\zeta_k = \zeta_l$ of a pair $l = \lambda(k)$ coincide, and squeeze a shorter slit S_i, i.e., $\omega(k) = i$ and $\omega(i) = l$. We have two thin sectors F_k and F_i, and the identifications declared on their four edges result in an interval attached at both ends to $F(L)$. Compared to Figure [25] the handle there degenerated to an interval here by making all meridians become points.

Note that this is very different from the configuration shown in Figure [11], where a pair of slits conincide and squeeze a longer slit. This surface is non-degenerate, and is built like in Figure [25], only that ζ_4 lies on the line labelled with a.

A limit case, namely a coinciding pair squeezing a slit of precisely the same

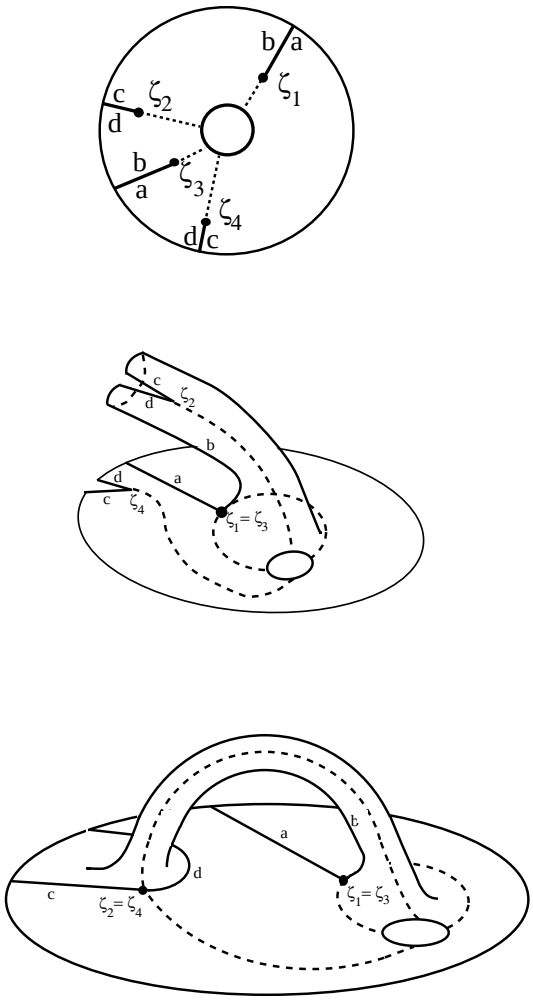

Figure 25: $n = 1, h = 2, m = 1, g = 1$ *: The first picture shows the configuration, the second an intermediate state of the gluing process, and the third picture shows a torus with two boundary curves.*

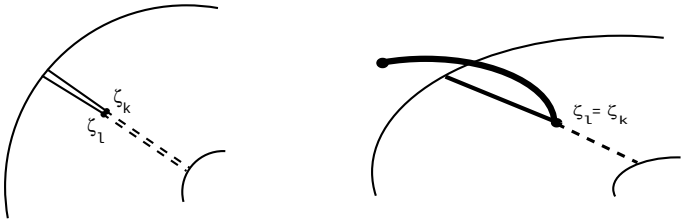

Figure 26: *A surface with a "thin" tube.*

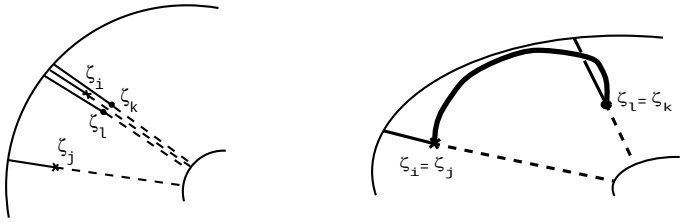

Figure 27: *A surface with a "thin" handle.*

length is shown in Figure [28]. It produces a surface with a cone singularity. It can be seen as a limit of degenerate surfaces as in Figure [27] where the length of the attached interval has converged to zero; or as the limit of non-degenerate surfaces as in Figure [11], where the lengths of the slits have become equal.

Figure 28: *A surface pinched at two points.*

The Figure [29] shows the case of a pair of endpoints lying on the outer circle of the same or of different annuli. In Figure [30] we see the case of a pair of endpoints lying on the inner circle of the same annulus, or of different annuli with the same radius.

In Figure [31] one slit endpoint of a pair lies on the inner circle of an annulus, with radius R_p, but the other endpoint lies in the interior of a different annulus of smaller radius $R_q < R_p$. Although the result is a non-degenerate surface, we will nevertheless exclude these cases as degenerate, since the harmonic function to be considered in section 6 will have singularities on the boundary.

Note that the five cases shown in Figures [26 — 30] are in a way elementary; in general, several such singulaities can accumulate at the same point, producing multiple cone points and also a graph (whose edges are degenerate tubes or handles).

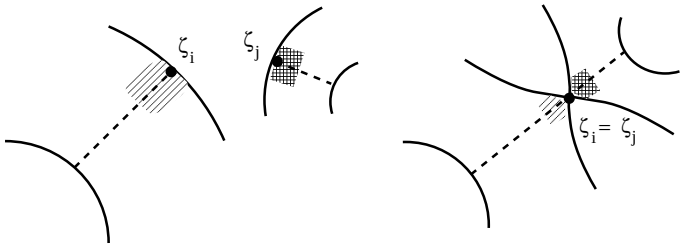

Figure 29: *A pair of endpoints lying on the outer circles of annuli.*

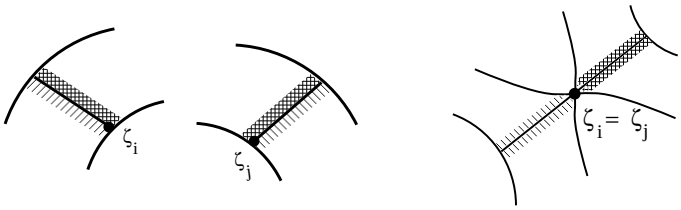

Figure 30: *A pair of endpoints lying on the inner circles of annuli .*

4.5 Criterion for Degeneracy

We will now investigate the question, for which configurations L the associated surface is $F(L)$ degenerate.

If $z = q_L(\bar{z})$ for some point $\bar{z} \in \bar{F}(L)$ in the interior of a proper sector F_k, then z is obviously a smooth point of $F(L)$, using the interior of F_k as coordinate chart.

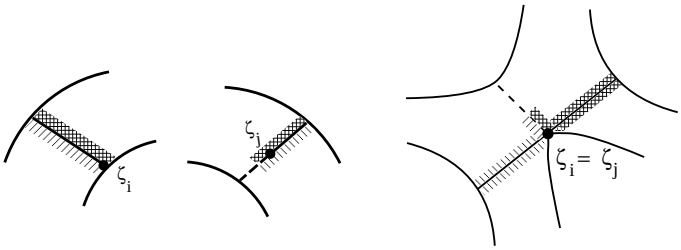

Figure 31: *One endpoint of a pair lies on an inner circle of an annulus, the other endpoint lies in the interior of another annulus.*

If $z = q_L(\bar{z})$ lies on the boundary $\partial F(L) = \partial^+ F(L) \cup \partial^- F(L)$ $\bar{z}$ lies on the interior of some curve $\gamma_k^{\pm}$ of a proper sector F_k, then z is also a smooth point of $F(L)$, using again the interior of F_k as a coordinate chart.

Let $z = q_L(\bar{z})$ be a point of $F(L)$ with modulus ξ; for the moment we assume that $\bar{z}$ does not lie on $\partial F(L)$. For this fixed ξ consider all $4h$ (not necessarily distinct) points of the form $(\xi, k, \pm)$, $k \in I$ and choose a closed neighbourhood $\bar{U}(\xi, k, \pm)$ in F_k as shown in Figures [32 — 35] : if $k \in \Xi$, then $\bar{U}(\xi, k, \pm)$ is an interval of length $2d$ with center $(\xi, k, \pm)$; otherwise $\bar{U}(\xi, k, \pm)$ is a half-disc of diameter $2d$ and with $(\xi, k, \pm)$ being the center of its left resp. right radial diameter. Here d is chosen small enough such that $\bar{U}(\xi, k, \pm)$ does not intersect the opposite edge of the sector F_k (if F_k is proper) and such that $\bar{U}(\xi, k, \pm)$ contains either no slit endpoint or precisely one (namely $(\xi, k, \pm)$ itself if it happens to be an endpoint).

Consider all $8h$ symbols $T(\pm, k, \pm)$, $k \in I$, and denote by $\mathcal{T}$ the subset for which $(\xi, k, \pm)$ is equivalent to $\bar{z}$, i.e., $(\xi, k, \pm) \in q_l^{-1}(z)$. Clearly, $T(\varepsilon, k, \pm)$ stands for the point $(\xi + \varepsilon d, k, \pm)$ in $\bar{U}(\xi, k, \pm) \cap E_k^{\pm}$. The images $U(\xi, k, \pm) = q_L(\bar{U}(\xi, k, \pm)$ for $(\xi, k, \pm) \in q_L^{-1}(z)$ unite to a neighbourhood $U(z)$ of z in $F(L)$; it is a cone over the boundary $\partial U(z) = \bigcup q_L(\partial \bar{U}(\xi, k, \pm)$ with cone point z.

On $\mathcal{T}$ we define a permutation $\Delta : \mathcal{T} \to \mathcal{T}$, which reflects the identifications

on the boundaries of all these neighbourhoods during the gluing.

$$
\begin{aligned}
(4.6) \qquad \Delta(T(+,k,-)) &= T(+,k,+), \text{ if } k \in \Xi \\
\Delta(T(-,k,+)) &= T(-,k,-), \text{ if } k \in \Xi \\
\Delta(T(+,k,-)) &= T(-,k,-), \text{ if } k \notin \Xi \\
\Delta(T(-,k,+)) &= T(+,k,+), \text{ if } k \notin \Xi \\
\Delta(T(+,k,+)) &= T(+,\omega(k),-), \text{ if } \xi + d < |\zeta_{\omega(k)}| \\
\Delta(T(-,\omega(k),-)) &= T(-,k,+), \text{ if } \xi + d < |\zeta_{\omega(k)}| \\
\Delta(T(+,k,+)) &= T(+,\kappa^{-1}(k),-), \text{ if } \xi - d > |\zeta_{\omega(k)}| \\
\Delta(T(-,\kappa^{-1}(k),-)) &= T(-,k,+), \text{ if } \xi - d < |\zeta_{\omega(k)}| \\
\Delta(T(+,k,+)) &= T(+,\kappa^{-1}(k),-), \text{ if } \xi = |\zeta_{\omega(k)}| \\
\Delta(T(-,\kappa^{-1}(k),-)) &= T(-,\lambda(k),+), \text{ if } \xi = |\zeta_{\omega(k)}| \\
\Delta(T(-,\omega(k),-)) &= T(-,k,+), \text{ if } \xi = |\zeta_{\omega(k)}|
\end{aligned}
$$

It follows that $U(z)$ is a disc if and only if $\partial U(z)$ is a single curve; and this is equivalent to the permutation Δ having exactly one cycle. The interior of $U(z)$ is then a coordinate chart.

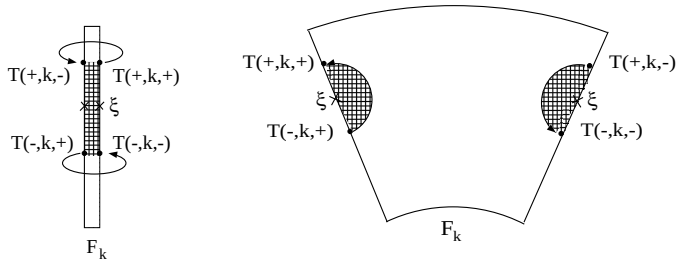

Figure 32: Δ *for a thin sector and a proper sector.*

The Figures [32 — 35] illustrate the permutation Δ on the points $T = T(\pm, k, \pm) = (\xi \pm d, k, \pm)$. Under the gluing T is identified with $T' = \Delta(T)$ and the cycle(s) of points $T, \Delta(T), \Delta^2(T), \ldots$ surrounds the point z in counterclockwise orientation on the boundary(s) of $U(z)$.

It will be convinient to give each endpoint ζ_k (or rather its image $z = q_L(\zeta_k)$ in $F(L)$ an *index*, defined to be one less than a quarter of the number of $T = T(\pm, l, \pm) \in \mathcal{T}$ such that $l \in I$, $l \notin \Theta$ and $q_L(\xi, k, \pm) = z$, where $\xi = |\zeta_k|$. For a smooth point ζ_k the number of half-discs forming the neighbourhood $U(z)$ is $2(\mathrm{ind}(\zeta_k) + 1)$.

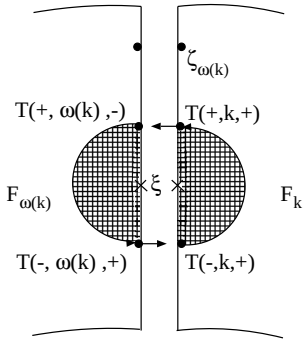

Figure 33: Δ *for* ξ *smaller than* $|\zeta_{\omega(k)}|$.

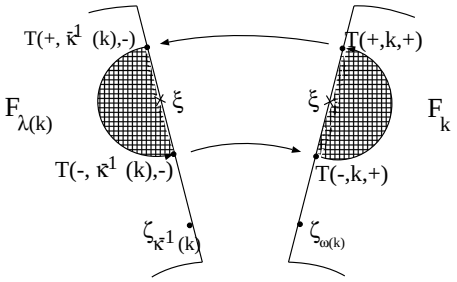

Figure 34: Δ *for* ξ *larger than* $|\zeta_{\omega(k)}|$.

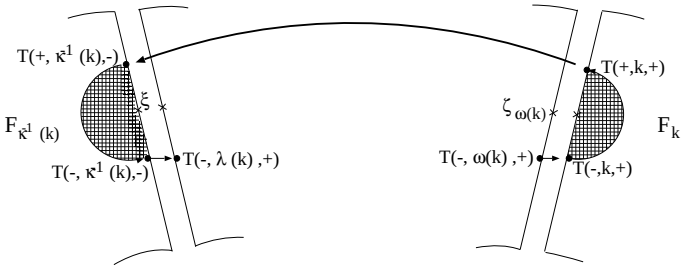

Figure 35: Δ *for* ξ *equal to* $|\zeta_{\omega(k)}|$.

If $z = q_L(\bar{z})$ and $\bar{z}$ lies in $E_k^{\pm} \cap \gamma_k^{\pm}$, a similiar criterion as above can be derived.

We call a configuration L *degenerate*, if $F(L)$ is degenerate, meaning it is not a topological surface or some endpoint is not in the interior of $\mathbb{B}$. The criterion we just formulated with the help of Δ is certainly violated, if L contains a subconfiguration of one of the five elementary types listed below. We have seen these five types in the Figures [26 — 30].

(4.7) There is some pair (i,j), i.e., $j=\lambda(i)$, in I with :
$\zeta_i=\zeta_j$ and $j=\omega(i)$,
$\zeta_i=\zeta_j$ and $k=\omega(i)$ and $j=\omega(k)$ and $|\zeta_k|>|\zeta_i|=|\zeta_j|$,
$\zeta_i=\zeta_j$ and $k=\omega(i)$ and $j=\omega(k)$ and $|\zeta_k|=|\zeta_i|=|\zeta_j|$,
ζ_i and thus ζ_j is in $\partial^+(\mathbb{B})$,
ζ_i or ζ_j is in $\partial^-(\mathbb{B})$.

The first three types can be comprised into one condition :

(4.8) There is some pair (i,j) in I, with $\nu(i)=\nu(j)=r$, $i\in\Xi$
and $\zeta_i=\zeta_j$ such that $|\zeta_k|\geq|\zeta_i|=|\zeta_j|$
for all $k\in I$ between i and j in the cyclic ordering of I_r.

The following lemma follows from the Δ-criterion. We shall see that the existence of a degenerate subconfiguration is not only sufficient, but essentially also necessary for L to be degenerate.

Lemma 4.1. *If L contains a subconfiguration of one of the types in (4.7), then L is degenerate.*

□

4.6 Non-degenerate Configurations

Assume $F(L)$ is not degenerate. The identifications $q_l:\bar{F}(L)\to F(L)$ leave the modulus $|\bar{z}|=\sqrt{\bar{x}^2+\bar{y}^2}$ of points $\bar{z}=\bar{x}+\sqrt{-1}\ \bar{y}$ unchanged, regardless of $\bar{z}$ being identified with points on the same or perhaps on other annuli. The coordinate charts we found above define therefore a canonical complex structure, because coordinate changes can be expressed by rotations in the the complex plane. It follows that $F(L)$ is orientable.

Lemma 4.2. *$F(L)$ has a canonical complex structure, if L is not degenerate.*

□

This answers question 4.2(b).

Lemma 4.3. *$F(L)$ is connected for all L.*

Proof. The connectedness of $F(L)$ is guaranteed by condition (3.11). □

Lemma 4.4. *$F(L)$ has $m+n$ boundary circles, if L is not degenerate.*

Proof. The boundary of $F(L)$ consists of all points on the curves $\gamma_1^-, \dots, \gamma_{2h}^-$ and $\gamma_1^+, \dots, \gamma_{2h}^+$. The pieces γ_i^- are glued together in the ordering given by ω, i.e., γ_i^- is followed by $\gamma_{\omega(i)}^-$, which is part of the next sector over the same annulus. Therefore all γ_k^- with k in some ω-cycle I_r form a boundary curve, and we have exactly n such. The pieces γ_i^+ are glued together in the ordering given by κ, i.e., γ_i^+ is followed by $\gamma_{\kappa(i)}^+$, which is perhaps part of a sector over a different annulus. Therefore all γ_i^+ with i in some κ-cycle form a boundary curve, and we have exactly m such. □

If L is degenerate, some of these boundary circles may be points. Note that the incoming and the outgoing boundary circles are numbered by the functions ν and μ, respectively. For each of the incoming boundary circles we take the real point $P_r = R_r \in \mathbb{A}_r$, $r = 1, \dots, n$, as marked point of $F(L)$.

Lemma 4.5. *The Euler characteristic of $F(L)$ is $\chi(F(L)) = -h$, if L is not degenerate.*

Proof. Assume first, that L is generic. Then each of the $2h$ sectors F_k in $\bar{F}(L)$ is proper and contributes to $F(L)$ the following : four corner points (each to be idetified one other corner point), the two endpoints ζ_k and $\zeta_{\omega(k)}$ (each to be identified with four other endpoints in $\bar{F}(L)$), the two curves $\gamma_k^\pm$, the two curves $\alpha_k^\pm$ and $\beta_k^\pm$ (each to be identified with one other such curve), and one planar piece. If we set $\chi_k = 4 \cdot \frac{1}{2} + 2 \cdot \frac{1}{4} - 2 - 4 \cdot \frac{1}{4} + 1 = -\frac{1}{2}$, we find

$$\chi(F(L)) = \sum_{k \in I} \chi_k = -\frac{1}{2} \cdot 2h = -h.$$

In a non-generic case $F(L)$ is obtained from a generic case by replacing a proper sector by a thin sector. This does dot change the Euler characteristic, as long as $F(L)$ remains non-degenerate. □

We finish this section with the remark that the function $u = u_L : F(L) \to \mathbb{R}$, $u(z) = \ln(|z|) = \Re(\ln(z))$ is always well-defined on the space $F(L)$, because of the modulus being invariant under the identifications. It has constant boundary value $\ln(R_0)$ on the outer curves and $\ln(R_i)$ on the inner curves. If L is non-degenerate, then u_L is harmonic with respect to the conformal structure of $F(L)$. (Note that u_L is also defined and continuous for degenerate L.) The zeroes of the gradient field Φ of u_L are precisely the endpoints ζ_k, and the indices are $\mathrm{ind}(\zeta_k)$ as defined above. For a generic L the function u_L is a Morse function.

5 The Reducible Presentation of a Configuration

Our next aim is to introduce a *reducible notation* for configurations. The result will actually not be a reduction in the notation, only a reduction in the number of slits, but at the expense of more data attached to each slit. The advantage lies firstly in the deletion of the ambiguities caused by jumps, as seen in Figure [9] above. And secondly will it make some proofs easier.
The idea is roughly to eliminate thin sectors by incoorperating the identifications on their right edge E_k^- into the identifications on the right bank of $F_{\omega(k)}$, and similarily with the left edge E_k^+. We will have fewer slits, but each bank of a slit may be subdivided into several intervals, each to be identified with another on some different edge.

5.1 Reducible Representations

Recall that g, m and n are given and that $h = 2g-2+m+n$. As before we use an *index set* I, but now of varying size $n \leq |I| \leq 2h$. There is a *distribution function* $\nu : I \to \underline{n}$ with non-empty *partial index sets* $I_r := \nu^{-1}(r)$ for all $r \in \underline{n}$. An *argument function* $\theta : I \to \mathbb{S}^1$ is given, and we use the notation S_k and S'_k for $k \in I$ as before. The *successor permutation* $\omega \in \mathfrak{S}(I)$ is now an element of the symmetric group of I. Its cycle $\langle k, \omega(k), \omega^2(k), \ldots \rangle$ is the *partial index set* $I_{\nu(k)}$. Furthermore, the cyclic ordering induced by ω on each I_r corresponds as before to the cyclic ordering of all endpoints on $\mathbb{A}_r$ by their argument, i.e., the argument function θ is monotone on each $I_1, \ldots, I_n$. As before we have a subset $\Xi \subset I$ of *exceptional indices* satifying (3.7) and (3.8). The notation S_k and S'_k will be used as before.
For the new presentation we need a *second index set* J with $4n \leq |J| \leq 8h$ elements. More precisely, to each $k \in I$ there are two non-empty, finite and linearly ordered sets J_k^+ and J_k^- associated; we set $J := \bigsqcup J_k^+ \sqcup \bigsqcup J_k^-$. We obtain a function $\iota : J \to I$ by $\iota^{-1}(k) = J_k^+ \sqcup J_k^-$. And we obtain a function

$\epsilon : J \to \{\pm 1\}$ by $\epsilon^{-1}(+1) = J^+$ and $\epsilon^{-1}(-1) = J^-$, respectively. Each $J_k^\pm$ will have at least two elements.
To each $j \in J$ there is a point $\zeta_j \in \mathbb{B}$ associated, such that

$$\zeta_j \in \mathbb{A}_{\nu(\iota(j))} \quad \text{for all } j \in J, \tag{5.1}$$

$$\arg(\zeta_j) = \theta(\iota(j)) \quad \text{for all } j \in J, \tag{5.2}$$

$$|\zeta_j| = R_{\nu(\iota(j))} \quad \text{if } j = \min(J_k^+) \text{ or } j = \min(J_k^-), \tag{5.3}$$

$$j \mapsto |\zeta_j| \text{ is weakly monotonic on } J_k^+ \text{ and } J_k^- \text{ for all } k \in I. \tag{5.4}$$

On the set J we are given a fix-point-free involution $\lambda \in \mathfrak{S}(J)$ satifying

$$\epsilon(\lambda(j)) = -\epsilon(j) \tag{5.5}$$

$$|\zeta_{\lambda(j)}| = |\zeta_j)| \tag{5.6}$$

The connectivity is again expressed in terms of a graph G as follows : the vertex set is $\underline{n}$, and there is an (undirected) edge between r_1 and r_2 if and only if there is some $j \in J$ with $\nu(\iota(j)) = r_1$ and $\nu(\iota(\lambda(j))) = r_2$. We demand that G is connected.
The *boundary exchange* $\kappa \in \mathfrak{S}(I)$ is given by $\kappa(i) := \iota(\lambda(\max(J^+_{\omega(i)})))$ for each $i \in I$. As before κ is supposed to have m cycles. And a numbering of its cycles is given as a κ-invariant function $\mu : I \to \underline{m}$.
A reducible presentation is written in double parantheses as

$$L = ((I, J, \zeta, \omega, \lambda, \Xi, \iota, \epsilon, \mu; R)). \tag{5.7}$$

Note that the functions ν and θ are determined by the function ζ. The permutation κ is determind by ω, λ, ι and the linear order in each $J_k^\pm$. The following diagram shows all the data occuring in the presentation.

(5.8)

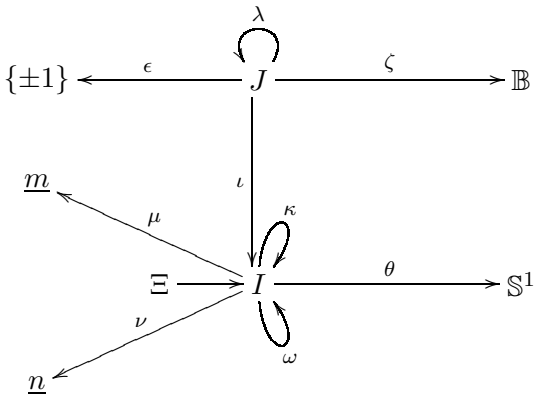

A presentation with $\Xi = \emptyset$ is called *reduced*. The reduced presentation of a configuration is unique.
After an example we describe the reduction procedure.

Example : As a first example we rewrite a configuration L presented in the old, unreducicble notation as $L = (\zeta; \lambda, \omega, \Xi; R)$. In both presentations the index set I is $\underline{2h}$, and we have the same distribution function ν, argument function θ and successor permutation ω, as well as the exceptional indicex set Ξ. The second index set is $J = \{(i, 0, \pm)|i \in I\} \cup \{(i, 1, \pm)|i \in I\}$ with $\iota(i, 0, \pm) = \iota(i, 1, \pm) = i$ and $\epsilon(i, 0, \pm) = \epsilon(i, 1, \pm) = \pm$. Thus each $J_k^{\pm}$ consists of the two elements $(k, 0, \pm)$ and $(k, 1, \pm)$. The pairing λ' on J is given by $\lambda'(i, 0, \pm) = (i, 0, \mp)$ and $\lambda'(i, 1, \pm) = (\lambda(i), 1, \mp)$. The function $\zeta' : J \to \mathbb{B}$ is $\zeta'(i, \pm) = \zeta_i$. It follows that we have the same κ as before; and we leave μ unchanged, as well the radii. Thus we arrive at $L = ((I, J, \zeta', \omega, \lambda', \Xi, \iota, \epsilon, \mu; R))$. Essentially we only quadrupled the index set I to get J. Obviously, this presentation is only reduced, if Ξ is empty.

5.2 Reduction

Let $j_1 < j_2 < \ldots < j_p$ be the elements of J_k^+ in their linear order; we denote by $\beta_{j_1}, \beta_{j_2}, \ldots, \beta_p$ the intervals on the right edge E_k^- of F_k between the consecutive points $\zeta_{j_1}, \zeta_{j_2}, \ldots, \zeta_{j_p}$ and $R_0\,\theta(k)$ on the outer boundary curve of the annulus $\mathbb{A}_{\nu(k)}$. And analogously we do this for the set $J_{\omega(k)}$, whose associated points subdivide the left edge E_k^+ of F_k.

To describe a reduction, let $k \in \Xi$ be an exceptional index, and set $l = \omega(k)$. Left and right edge of this thin sector F_k agree and we write $E = E_k^+ = E_k^-$. This E is twice divided into intervals β_j, one division is induced by J_k^+, and one by J_l^-. Consider the common subdivision they induce on E and in particular some β_j, say for example $j \in J_l^-$. Each subinterval of β_j has now two labels associated, namely j and some $j' \in J_k^+$. We transport the subdivision of β_j to $\beta_{\lambda(j)}$, together with the label j'.
In the Figures [36 and 37] we labelled only some intervals by their indices $j_1, \ldots, j_4$, giving paired intervals the same label. In both Figures a reduction is shown.
The index k is deleted from I. We keep J_l^+, but replace J_l^- by J_k^-, furthermore, for each j as above we replace the single element $\lambda(j)$ in $J_{\iota(\lambda(j))}$ by the elements written as pairs (j, j') for all j' as above, linearly ordered by their modulus. The pair (j', j) will occur in this way as a new element in $J_{\iota(\lambda(j'))}$, and (j, j') and (j', j) will be paired. Figure [37] shows the reduction of [36].

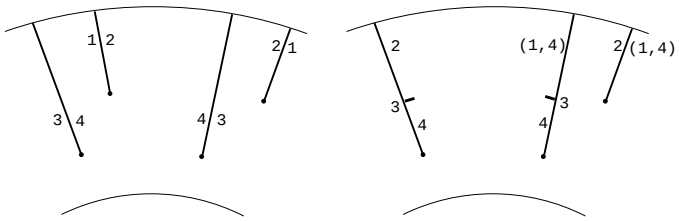

Figure 36: *A reduction.*

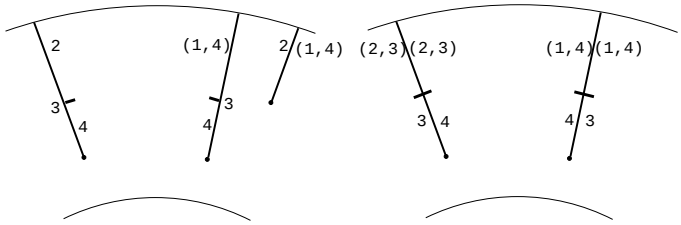

Figure 37: *A further reduction.*

There is another reduction step : If for two consecutive $j_1 < j_2$ in $J_l^{\pm}$ the paired indices $\lambda(j_1)$ and $\lambda(j_2)$ are in the same $J_{l'}^{\mp}$, then j_2 and $\lambda(j_2)$ is cancelled from $J_l^{\pm}$ and $J_{l'}^{\mp}$, respectively. This corresponds to an amalgamation of β_{j_1} with β_{j_2} and of $\beta_{\lambda(j_1)}$ with $\beta_{\lambda(j_2)}$ which are adjacent intervals on ideal boundary edges.

6 The Configuration Associated to a Surface

We have seen in section 4 how to associate to a configuration L a (possibly degenerate) surface $F(L)$. In this section we show how to associate a configuration L to a given Riemann surface F of genus g and $m+n$ boundary curves $C_1^-, \ldots C_n^-, C_1^-, \ldots C_m^+$ with marked points $P_i \in C_i^-$, $P = (P_1, \ldots, P_n)$. Let $C^+ = C_1^+ \cup \ldots \cup C_m^+$, $C^- = C_1^- \cup \ldots \cup C_n^-$ and $C = C^+ \cup C^-$. As before set $h = 2g + m + n$.

6.1 Harmonic Potentials

Let

$$u_F = u : F \to \mathbb{R} \tag{6.1}$$

be a harmonic function which has no singularities, all its critical points in the interior, and which is constant on the boundary curves; we set it equal to 0 on the incoming boundary C^- and equal to some constant $c_j < 0$ on the outgoing boundary curve C_j^+, $j = 1, \ldots, m$. Such a function, a solution of the Dirichlet problem, always exists and is uniquely determind by the complex structure and the boundary values; see e.g. [C], [F, p.164].
If we set (as we will do later in section 9) $c_1 = \ldots = c_m = c$, then u exhibits F as a harmonic, and therefore smooth bordism between C^+ and C^- over the interval $[c, 0]$.

Let $\Phi = \mathrm{grad}(u)$ denote the gradient vector field. (For this we need to choose a metric in the conformal class of F; but we will only use properties of Φ which are independent of the choice of the metric in this conformal class.) The vector field Φ has no singularities and its zeroes $Z_1, \ldots, Z_s$, i.e., the critical points of u, lie in the interior of F. Since u is locally the real part of a holomorphic function, the zeroes will be saddle points of some index and $-2h \leq \mathrm{ind}(Z_k) \leq -1$. Note that u is in general not a Morse function, since it might have degenerate critical points. The sum of these indices must be the Euler characteristic $\chi(F) = -h = 2 - 2g - m - n$, thus s is bounded by $0 \leq s \leq h$. Unless $n = m = 1$ and $g = 0$ (i.e., unless F is an annulus), there is at least one zero.

6.2 Critical Graphs

Consider a single zero Z_i of index $-p$. It has $p+1$ *stable* flow lines entering and $p+1$ *unstable* flow lines leaving. Each stable flow line either comes from another zero Z_j or from some boundary point $Q^- \in C^-$. And each unstable flow line either goes to another zero Z_k or to a boundary point $Q^+ \in C^+$. We call these points $Q^\pm$ on $C^\pm$ the *cut points* of F.

The *critical graph* $\mathcal{K}$ of F consists of all cut points and all zeroes as vertices, and its edges are the flow lines (stable or unstable) connecting two vertices. All edges are oriented by the flow Φ. Since $\mathcal{K}$ is embedded in an oriented surface, all edges entering (resp. leaving) vertices (i.e., zeroes) are cyclically ordered; furthermore, entering and leaving edges alternate. The valency of a vertex is 1 for a cut point Q, and $-2\,\mathrm{ind}(Z_i) + 2$ for a zero Z_i. Note that there may be several edges connecting the same two zeroes. On each boundary curve there is at least one cut point, unless F is an annulus.

Let $\check{\mathcal{F}} = F \setminus \mathcal{K}$ be the complement of the critical graph, and let $\check{\mathcal{F}}_k$ denote a component of $\check{\mathcal{F}}$, where k ranges over some index set I. A component

$\check{\mathcal{F}}_k$ intersects C^- as well as C^+. The gradient vector field Φ has no singularities on $\check{\mathcal{F}}_k$ and can therefore be used to retract $\check{\mathcal{F}}_k$ backwords onto the intersection $\check{\mathcal{F}}_k \cap C^-$.
Thus $\check{\mathcal{F}}_k$ is either homotopy equivalent to an open interval and thus contractible (in case $\check{\mathcal{F}}_k \cap C^-$ is a proper part of some boundary curve), or $\check{\mathcal{F}}_k$ is homotopy equivalent to $\mathbb{S}^1$ (in case $\check{\mathcal{F}}_k \cap C^-$ is an entire boundary curve). The second case can only occur, when there are no cut points at all; then $\mathcal{K}$ is empty, i.e., F is an annulus and the only component.

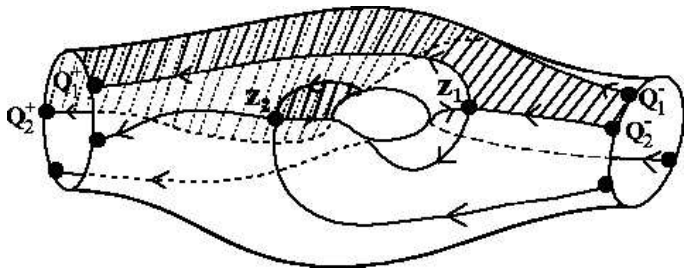

Figure 38: *The critical graph of a surface with $g = 1$, $n = m = 1$.*

In the Figures [38] and [39] we show the critical graph $\mathcal{K}$ of a potential of a generic surface with $g = 1$ and $n = m = 1$. One of the four components of the complement of $\mathcal{K}$ is shaded and shown in Figure [39] separatedly.

Looking at a fixed incoming circle C_r^- $(r = 1, \ldots, n)$, the set of those components $\check{\mathcal{F}}_k$ which intersect the boundary curve C_r^- non-trivially inherits from the counterclockwise orientation a cyclic ordering. Let this ordering be described by a permutation $\omega \in \mathfrak{S}(I)$, i.e., its cycles are the sets $I_r = \{i \in I \mid \check{\mathcal{F}}_k \cap C_r^- \neq \emptyset\}$ for $r \in \underline{n}$.

On each $\check{\mathcal{F}}_k$ the harmonic function $u_k := u|\check{\mathcal{F}}_k : \check{\mathcal{F}}_k \to \mathbb{R}$ is the real part of a holomorphic function

$$w_k = u_k + \sqrt{-1}\, v_k : \check{\mathcal{F}}_k \longrightarrow \mathbb{C} \tag{6.2}$$

where v_k is the harmonic conjugate of u_k and is unique up to an additive constant d_k. Since v_k is constant along the gradient flow lines of u_k, which are the boundary of $\check{\mathcal{F}}_k$ in F, the image of w_k is the open rectangle $[0,1]\times]a_k, b_k[$ for some $a_k < b_k$.
If we add to each level set $M_k(x) := \{z \in F | u(z) = x\}$, $x \in [0,1]$, two endpoints ξ_x^0, ξ_x^1, we obtain $\mathcal{F}_k$ as the ideal closure of $\check{\mathcal{F}}_k$. Setting $u_k(\xi_x^0) =$

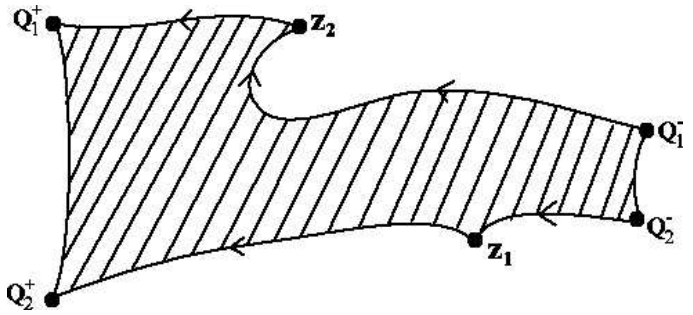

Figure 39: *A component of the complement of the critical graph.*

$u_k(\xi_x^1) = x$ and $v_k(\xi_x^0) = a_k$, $v_k(\xi_x^1) = b_k$ extends w_k, and the image is the closed reactangle $[0,1] \times [a_k, b_k]$. There is a map $q_F : \bigsqcup_{k\in I} \mathcal{F}_k \to F$, and this map is an embedding on each $\check{\mathcal{F}}_k$. The preimage $q^{-1}(Z_i)$ consists of $2\,\mathrm{ind}(Z_i) + 2$ ideal boundary points.

6.3 Uniformization

We arrange these constants d_k in the following way. For $r \in \underline{n}$ pick $k \in I$ such that $P_r \in q_F(\mathcal{F}_k)$, and write $I_r = \langle k, \omega(k), \omega^2(k), \ldots\rangle$. Then choose $d_k, d_{\omega(k)}, d_{\omega^2(k)}, \ldots$ such that

(1) $v_k(P_r) = 0$,

(2) $b_k = a_{\omega(k)}$, $b_{\omega(k)} = a_{\omega^2(k)}$, and so on.

The images $w_k(\mathcal{F}_k)$ for $k \in I_r$ cover a rectangle $[0,1] \times [a,b]$ with $b - a = \sum_{k\in I_r} b_k - a_k$. A dilation with factor $c = \frac{2\pi}{b-a}$ and a translation about c to the left gives the rectangle $[-c, 0] \times [c\,a, c\,b]$ with the same modulus $b - a$. We then define

$$W_k(z) = \exp(w_k(z)) : \mathcal{F}_k \longrightarrow \mathbb{C}. \tag{6.3}$$

The image of W_k is a sector of an annulus $\mathbb{A}_r$ with inner radius $R_r = \exp(-c_r)$, and outer radius $R_0 = \exp(0) = 1$, and with angular width $\exp(\sqrt{-1}(b_k - a_k))$.

Obviously, we have arrived at a reduced description of a configuration L. The index sets $J_k^{\pm}$ are the ideal boundary points of $\mathcal{F}_k$ lying over zeroes or cut points on C^-, i.e., $J_k^- = q_F^{-1}(\mathcal{K}') \cap v_k^{-1}(a_k) \subset \mathcal{F}_k$ and $J_k^+ = q_F^{-1}(\mathcal{K}') \cap v_k^{-1}(b_k) \subset \mathcal{F}_k$, where $\mathcal{K}'$ are the vertices of $\mathcal{K}$ which are not cut points on

C^+. These sets are lineraly ordered by increasing values of u. The edges of $\mathcal{K}$ induce a division of the two ideal boundary edges of $\mathcal{F}_k$ into intervals. Since they are identified in pairs, a pairing on $J = \bigsqcup_{k\in I} J_k^{\pm}$ is established. This answers question 4.2(c).

For the suface of Figure [38] the resulting configuration is as shown in Figure [6].

7 The Configuration Spaces $\mathfrak{Rad}_h(m,n)$

The configurations $L = (\zeta; \lambda, \omega, \Theta; R)$ introduced in section 3.1 are regarded as points in the space $\mathbb{B}^{2h} \times \mathfrak{S}_{2h} \times \mathfrak{S}_{2h} \times \{0,1\}^{2h} \times]0,\infty[^{n+1}$ satisfying the conditions (3.1) to (3.13); we denote this subspace by $\mathrm{Conf}_h(m,n)$. To answer question 4.2(d) we will show that $F(L)$ does not depend on the numbering of the endpoints, is invariant under jumps and under dilations of the annuli.

7.1 Renumbering

To be precise, let $\sigma \in \mathfrak{S}_{2h}$ be a renumbering of the index set I and set $\zeta^\sigma := (\zeta_{\sigma(1)}, \ldots, \zeta_{\sigma(2h)})$, $\lambda^\sigma := \sigma \circ \lambda \circ \sigma^{-1}$, $\omega^\sigma := \sigma \circ \omega \circ \sigma^{-1}$, $\Theta^\sigma := \sigma(\Theta) = \{\sigma(k) \mid k \in \Theta\}$. Then we set $L^\sigma := (\zeta^\sigma; \lambda^\sigma, \omega^\sigma; R)$. Note that the former distribution function $\nu : I \to \underline{n}$ is replaced by the new $\nu^\sigma := \nu \circ \sigma$, and the former boundary exchange κ by the new $\kappa^\sigma := \sigma \circ \kappa \circ \sigma^{-1}$.

Lemma 7.1.
There is a homeomorphism $F(L) \to F(L^\sigma)$, which is a conformal equivalence for non-degenerate L.

Proof. The homeomorphism is induced by the identity on each of the sectors $F_k(L) = F_{\sigma(k)}(L^\sigma)$. □

7.2 Jumps

We have also seen that a shorter slit jumping over a longer pair does not effect $F(L)$. To describe this precisely, let k be in Θ, and set $i = \omega(k)$ and $j = \lambda(i)$. We say that k *jumps over the pair* (i,j) when we replace L by $L' = (\eta'; \lambda, \omega', \Theta'; R)$ where $\zeta' = (\zeta_1, \ldots, \zeta_k \frac{\zeta_j}{|\zeta_j|}, \ldots, \zeta_{2h})$ leading to the new distribution function ν' with $\nu'(k) = \nu(j)$ and $\nu'(l) = \nu(l)$ for $l \neq k$, where λ is unchanged, $\omega' := \langle k, \omega(j)\rangle \circ \omega \circ \langle k, \omega^{-1}(i)\rangle$, $\Theta' := (\Theta - \{k\}) \cap \{j\}$, and R is unchanged. Note that κ is replaced by $\kappa' := \lambda \circ \langle k, \omega(j)\rangle \circ \omega \circ \langle k, \omega^{-1}(i)\rangle$, which has the same number of cycles as κ; thus $m' = m$.

Lemma 7.2.
There is a homeomorphism $F(L) \to F(L')$, which is a conformal equivalence for nondegenerate L.

Proof. The homeomorphism is induced by the identity on each of the proper sectors. The thin sector F_k is identified with ideal boundary edges of proper sectors, on which the map agrees. □

These jumps make the space $\mathrm{Conf}_h(m,n)$ connected. In Figure [40] we see five stages of a closed curve in the space $\mathrm{Conf}_h(m,n)$, the first and the last picture agree. Only the slit S_2 is moving counterclockwise, between picture three and picture four it jumps over the pair $1 = \lambda(3)$. This curve represents — as an element of the fundamental group of $\mathfrak{M}_1^\bullet(1,1)$ — a Dehn twist.

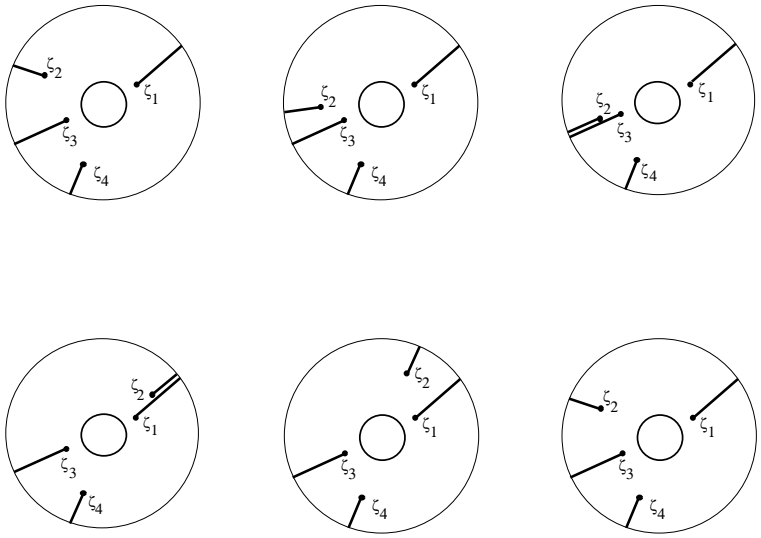

Figure 40: *$n = 1, h = 2, m = 1, g = 1$: A motion picture in 5 stages shows a path in the space $\mathfrak{Rad}_2(1,1)$; all slits are fixed except S_2, which moves counterclockwise towards S_3, jumps to S_1, and moves back to its former position.*

7.3 Dilations

Finally, we can obviously dilate all annuli $\mathbb{A}_1, \ldots, \mathbb{A}_n$ simultaniously by a positive real number a, replacing ζ by $a.\zeta = (a.\zeta_1, \ldots, a.\zeta_{2h})$ and R

by $a.R = (aR_0, aR_1, \ldots, aR_n)$. We denote this replacement by $a.L = (a.\zeta; \lambda, \omega, \Theta; a.R)$. Because of the connectivity condition (3.11), we can not dilate the annuli independently. Furthermore, since we have chosen the marked points P_i to be the real points $z = (R_i, 0)$, we can not rotate the annuli.

Lemma 7.3.
There is a homeomorphism $F(L) \to F(a.L)$, which is a conformal equivalence for non-degenerate L.

Proof. The homeomorphism is induced by sending z to az on each sector. □

7.4 $\mathfrak{Rad}_h(m,n)$

To replace a configuration L by L^σ for $\sigma \in \mathfrak{S}_{2h}$ or by $a.L$ for $a > 0$ or to perform a jump generates an equivalence relation $\approx$ on $\mathrm{Conf}_h(m,n)$; we denote an equivalence class by $\mathcal{L} = [L]$ and define $\mathrm{Rad}_h(m,n) = \mathrm{Conf}_h(m,n)/\approx$. Renumbering configurations and rescaling configurations is obviously an action by the group $\mathfrak{S}_{2h} \times \mathbb{R}_{>0}$; furthermore, instead of dividing by the action of $\mathbb{R}_{>0}$ we can normalize the outer radius to be $R_0 = 1$.

As we have seen in section 4 some configurations L yield singular surfaces $F(L)$. We call a class $\mathcal{L}$ *degenerate* if it contains any degenerate configuration.

Proposition 7.4.
$F(\mathcal{L})$ is degenerate if and only if $\mathcal{L}$ is degenerate.

Proof. By Lemma 4.1 the condition is sufficient. Assume Δ has for some point $\bar{z} = (\xi, k, \pm)$ more than one cycle in the set $\mathcal{T}$. Then by performing jumps of slits with index in those two cycles one can find a degenerate configuration in the class $\mathcal{L}$. □

Let $\mathfrak{Conf}_h(m,n)$ be the subspace of $\mathrm{Conf}_h(m,n)$ of all non-degenerate configurations, and set $\mathfrak{Rad}_h(m,n) = \mathfrak{Conf}_h(m,n)/\approx$.

Proposition 7.5. *The space $\mathfrak{Rad}_h(m,n)$ is a non-compact manifold of dimension $6h+n$.*

Proof. We sketch the proof, using induction on h. For $h = 2$ (and $n = 1$ or $n = 2$) the statement follows from the Examples above.

Let $\mathfrak{Rad}'_h(m,n)$ denote the space of $h+1$ pairs of radial slits, exactly as in $\mathfrak{Rad}_{h+1}(m,n)$, but one pair is *special* in the sense that its slits can jump over the other (ordinary) pairs (if shorter or of equal length), but a slit of an ordinary pair is not allowed to jump over the special pair.
There is a well-defined map $\phi : \mathfrak{Rad}'_h(m,n) \to \mathfrak{Rad}_h(m,n)$ forgetting the special pair. The map ϕ is surjective, but not open. Over the open set of generic configurations in $\mathfrak{Rad}_h(m,n)$ it is fibre bundle with fibre the configuration space of two (unordered) points ζ', ζ'' in $\mathbb{B} \setminus \bigcup_{k\in I}(S'_k \setminus S_k)$ of the same modulus $|\zeta'| = |\zeta''|$. If we introduce ideal boundary and use the induction hypothesis for $\mathfrak{Rad}_h(m,n)$, one can show that $\mathfrak{Rad}'_h(m,n)$ is a manifold with boundary.
Consider the map $\psi : \mathfrak{Rad}'_h(m,n) \to \mathfrak{Rad}_{h+1}(m,n)$, which ignores the nature of the special pair and regards it as ordinary. Now ψ is surjective (and a covering over the generic configurations) and identifies points on the boundary pairwise. Since these identifications are affine, we conclude that $\mathfrak{Rad}_{h+1}(m,n)$ is a manifold. □

7.5 Hilbert Uniformization

Summing up section 3 and 6 we have maps

$$\mathcal{G} \;:\; \mathfrak{Rad}_h(m,n) \to \mathfrak{M}^\bullet_g(m,n), \quad [L] \mapsto [F(L), P(L)] \tag{7.1}$$

$$\mathcal{H} \;:\; \mathfrak{M}^\bullet_g(m,n) \to \mathfrak{Rad}_h(m,n), \quad [F,P] \mapsto [L(F)]. \tag{7.2}$$

We call $\mathcal{H}$ the *Hilbert uniformization.* Obviously we have

Proposition 7.6.
$\mathcal{H} \circ \mathcal{G} = \mathrm{id} : \mathfrak{Rad}_h(m,n) \to \mathfrak{M}^\bullet_g(m,n) \to \mathfrak{Rad}_h(m,n)$ *is the identity.*

Proof. The harmonic potential of $F = \mathcal{G}([L])$ is the function $u(z) = \ln(|z|)$ mentioned at the end of Section 4. The zeroes of the gradient flow Φ are the slit endpoints, and the critical graph if $\mathcal{K} = \bigcup S'_k$. The components $\mathcal{F}_k$ of the complement $F \setminus \mathcal{K}$ are the proper sectors of L. It is obvious that the composition $\mathcal{H} \circ \mathcal{G}$ sends a configuration to its reduced representation. □

Proposition 7.7.
$\mathcal{G} \circ \mathcal{H} = \mathrm{id} : \mathfrak{M}^\bullet_g(m,n) \to \mathfrak{Rad}_h(m,n) \to \mathfrak{M}^\bullet_g(m,n)$ *is the identity.*

Proof. The conformal maps W_k send a component $\mathcal{F}_k$ to a sector F_k of $L = \mathcal{H}([F])$. When composed with $q_L : \bar{F}(L) \to F(L)$, they agree along $\mathcal{K}$. Thus they yield a conformal equivalence $F \to F(L)$. □

Proposition 7.8.
$\mathcal{G} : \mathfrak{Rad}_h(m,n) \to \mathfrak{M}_g^\bullet(m,n)$ *is continuous.*

Proof. Let $\mathcal{L} = [L] \in \mathfrak{Rad}_h(m,n)$ be given. We need to find a quasi-conformal map $f : F(L) \to F(L')$ such that its maximal dilatation $K[f]$ can be bounded from above by a given $\epsilon > 0$, if L' is closer to L than some δ (depending on L and ϵ).
First consider the case, where the reduced representation of L and L' differ only in their functions ζ and ζ', or in their radii R and R', respectively, but not in their combinatorial data. Then they have the same number of proper sectors, and we can find a correspondence between these sectors, provided L and L' are so close to rule out symmetries of the configuration. Corresponding sectors can obviously be mapped onto each other by an homeomorphism $f_k : F_k \to F'_{k'}$ which is affine in polar coordinates. These homeomorphisms can be made to coincide along the ideal boundary edges. Their maximal dilatation $K[f_k]$ depends only on the difference of the angular width of F_k and $F'_{k'}$ and on the difference of the radii of the annuli involved. Both differences can be controlled by an appropriate δ.
Secondly, if the L' has in addition different combinatorial type than L, we can assume, that L' is the result of contracting a sector F_k of small angular width to a thin sector (and reducing). Consider the example in Figure [41]. The homeomorphism f maps the left and right half of F_k as indicated, winding it around all points ζ_j for $j \in J^{\pm}_{\omega(k)}$ after the reduction. The neighbouring sectors must also be adjusted. The maximal dilation of such a map depends only on the angular width of F_k and the index of the ζ_j. Thus it can be controlled by choosing an appropriate δ. □

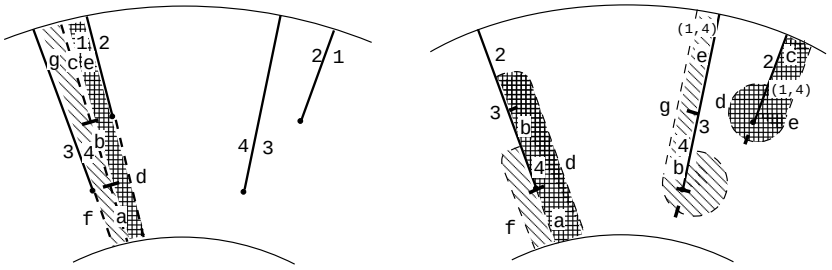

Figure 41: *The quasi-conformal map caused by a reduction.*

Proof of Theorem 1.1

Proof. The map $\mathcal{G}$ is continous and injective. Since the spaces $\mathfrak{Rad}_h(m,n)$ and $\mathfrak{M}_g^\bullet(m,n)$ are manifolds, it follows from the invariance of domain that $\mathcal{G}$ is an open map. □

The torus group $\mathbb{T}^n$ acts on $\mathfrak{Rad}_h(m,n)$ by rotating the n annuli independently, and on $\mathfrak{M}_g^\bullet(m,)$ by rotating each marked point P_i independently around its curve C_i^-. With these actions $\mathcal{G}$ and $\mathcal{H}$ are both equivariant. Thus a homeomorphic model of the (unmarked) moduli space $\mathfrak{M}_g(m,n)$ is obtained by dividing out the $\mathbb{T}^n$-action on $\mathfrak{Rad}_h(m,n)$.

7.6 Examples

Let us consider some examples.

Example 1. The space of all empty configurations $\mathfrak{Rad}_0(1,1)$ consists of all classes of configurations $L = (-;-,-;(R_0,R_1))$, thus normalizing $R_0 = 1$ we have a homeomorphism $\mathfrak{Rad}_0(1,1) \cong]0,1[$ by sending L to R_1/R_0. This ratio of outer and inner radius is the only modulus of an annulus and thus $]0,1[$ is as expected the moduli space $\mathfrak{M}_0^\bullet(1,1)$ of annuli. Note that it is the only case with a (continuous) group of conformal equivalences, which act transitively on all possible choices of marked points. Therefore $\mathfrak{M}_0^\bullet(1,1) = \mathfrak{M}_0(1,1)$.

Example 2. The next space $\mathfrak{Rad}_1(2,1)$ consists of the classes of configurations of two endpoints ζ_1, ζ_2 in one annulus, i.e., the configuration space of two unordered and distinct points on a circle (which is an open Möbius band $M = \mathbb{R}P^2 - \{\text{point}\}$), and their modulus $0 < |\zeta_1| = |\zeta_2| < 1$, and the inner radius $0 < R_1 < 1$. Thus $\mathfrak{M}_0^\bullet(2,1) \cong M \times]0,1[\times]0,1[$.

Example 3. The space $\mathfrak{Rad}_1(1,2)$ consists of configurations with two endpoints on two different annuli. Thus $\mathfrak{Rad}_0(1,2)$ is homeomorphic to $\mathbb{S}^1 \times \mathbb{S}^1 \times [0,1] \times [0,1]^2$.

Note that in example 2 and 3 the surfaces are pair-of-pants. The difference is caused by the number of marked points.

8 The Compactification $\mathrm{Rad}_h(m,n)$

The moduli spaces of surfaces with or without additional data like boundaries or punctures can be described by methods of various parts of mathematics, like complex analysis, real analysis, algebraic geometry, differential geometry, hyperbolic geometry or topology. But each description leads to

its own compactification by including some sorts of degenerate surfaces — usually by letting (local) parameters go to zero or to infinity. As a result, the compactifications do widely differ from each other.

8.1 Harmonic Compactification

The method of Hilbert uniformization used here to describe $\mathfrak{M}_g^\bullet(m,n)$ by its homeomorphic model $\mathfrak{Rad}_h(m,n)$ with $h = 2g-2+m+n$ leads to a compactification with the following characteristics : the degenerate surfaces $F(\mathcal{L})$ still admit a function $u : F(\mathcal{L}) \to \bar{\mathbb{R}} = \mathbb{R} \cup \infty$ which is harmonic at all smooth points of $F(\mathcal{L})$.

The space $\mathrm{Rad}_h(m,n)$ was introduced in section 7 as a quotient of the space $\mathrm{Conf}_h(m,n)$. Starting vice versa from the space $\mathfrak{Conf}_h(m,n)$, whose quotient is $\mathfrak{Rad}_h(m,n)$, we drop the conditions (a) to (e) and allow the inner radii $R_1, \ldots, R_n$ to vary between 0 and R_0; recall that we have fixed $R_0 = 1$.

$$\begin{array}{ccc} \mathfrak{Conf}_h(m,n) & \longrightarrow & \mathrm{Conf}_h(m,n) \\ \downarrow & & \downarrow \\ \mathfrak{Rad}_h(m,n) & \longrightarrow & \mathrm{Rad}_h(m,n) \end{array}$$

Since $\mathrm{Conf}_h(m,n)$ is a closed subspace of $\mathbb{B}^{2h} \times \mathfrak{S}_{2h} \times \mathfrak{S}_{2h} \times \{0,1\}^{2h} \times [0,1]^n$, it is compact; and consequently $\mathrm{Rad}_h(m,n)$ is compact as well. Its subspace $\mathfrak{Rad}_h(m,n)$ is open and dense.

The compactification adds degenerate surfaces to $\mathfrak{M}_g^\bullet(m,n)$. The degenerations occuring are of three types:
(a) a hande degenerates into an interval;
(b) a non-separating curve is pinched to a point;
(c) finitely many points are identified.
See the Figures [26 – 31] for examples. Such a degenerate surface is always a union of a non-degenerate surface of lower genus or with fewer boundary curves and a graph (whose edges are degenerate handles).

8.2 Cell Structure

To see the cell structure on $\mathrm{Rad}_h(m,n)$ we use the reduced description. A cell of $\mathrm{Rad}_h(m,n)$ consists of all classes $\mathcal{L} = [L]$ of configurations such

that their combinatorial data in the reduced presentation agrees and they differ only in the function ζ and the radii. The coordinates of such a cell are the $\theta(i)$ for $i \in I$, the moduli $|\zeta_j|$ for $j \in J$, and the radii $R_1, \ldots, R_n$. Each ω-cycle determines a simplex with the numbers $\theta(i)$ as barycentric coordinates. Then the numbers $|\zeta_j| = |\zeta_{\lambda(j)}|$ determine a simplex, and the radii $R = (R_0, R_1, \ldots, R_n)$ determine a cube. A cell is then a product of these spaces.

9 The Operad Structure

9.1 Composition of two Surfaces

The uniformization method described here makes the process of gluing (or composing) two surfaces along boundary curves particularily easy. Two arcs of equal length on two circles of equal radius in a complex plane, can – after a rotation and translation – be identified such that this extends to a conformal gluing of regions (locally) bounded by those arcs. If we identfy two circles in this way, such that two marked points are identified, there is preisely one such identification.

We therefore need to specify not only on each incoming boundary curve C_i^- of the surface F a marked point $P_i^- = P_i$, $(i = 1, \ldots, n)$, but also on each outgoing curve C_j^+ a marked point P_j^+, $(j = 1, \ldots, m)$. We shall denote the moduli space of theses surfaces by $\mathfrak{M}_g^{\bullet\bullet}(m, n)$. The new space $\mathfrak{M}_g^{\bullet\bullet}(m, n)$ is a $\mathbb{T}^m$-bundle over $\mathfrak{M}_g^{\bullet}(, n)$, which in turn is a $\mathbb{T}^n$-bundle over $\mathfrak{M}_g(m, n)$; see 2.4.

To make things as easy as possible we shall furthermore insist on all inner radii being equal, $R_1 = \ldots = R_n$. (Recall that the outer radius was set equal to $R_0 = 1$ in 7.4.) We denote this subspace $N\mathfrak{M}_g^{\bullet\bullet}(m, n)$, and note that it is a homotopy retract of $\mathfrak{M}_g^{\bullet\bullet}(m, n)$.

The corresponding space of non-degenerate radial slit configurations is denoted by $N\mathfrak{Rad}_g^{\bullet}(m, n)$. Note that a new marked point P_j^+ performs jumps if it moves continously around the boundary curve. Recall that the marked points P_i^- on the incoming curves C_i^- correspond in the slit configuration to the point $z = (R_i, 0)$, the intersection of the positive real axis with the inner boundary of the annuli.

The connected-sum-operation

$$\sharp : N\mathfrak{M}^{\bullet\bullet}_{g'}(m',m) \times N\mathfrak{M}^{\bullet\bullet}_{g}(m,n) \rightarrow N\mathfrak{M}^{\bullet\bullet}_{g'+g}(m',n) \tag{9.1}$$

$$(F',F) \mapsto \tilde{F} = F' \sharp F \tag{9.2}$$

will be described on the configuration spaces ($h = 2g - 2 + m + n$)

$$\sharp : N\mathfrak{Rad}^{\bullet}_{h'}(m',m) \times N\mathfrak{Rad}^{\bullet}_{h}(m,n) \rightarrow N\mathfrak{Rad}^{\bullet}_{h'+h}(m',n) \tag{9.3}$$

$$(\mathcal{L}',\mathcal{L}) \mapsto \tilde{\mathcal{L}} = \mathcal{L}' \sharp \mathcal{L} \tag{9.4}$$

and is defined in the following steps. Let the classes $\mathcal{L}$ resp. $\mathcal{L}'$ be represented by the configurations L resp. L'.

(1) First choose on n disjoint complex planes n annuli $\tilde{\mathbb{A}}_1, \ldots, \tilde{\mathbb{A}}_n$ of inner radius $R_1 = \ldots = R_n$ (the inner radius of L) and outer radius $\tilde{R}_0 = R_0 R'_0 / R'_1$. Into these annuli we will insert L as well as L'. At the very end we shall rescale the configuration and make the outer radius equal to 1.
(2) Insert the configuration L to these new annuli by putting it to the inner half (between radius R_1 and R_0) and prolonging its slits outward to the radius $\tilde{R}_0$.
(3) Rescale the m annuli $\mathbb{A}'_1, \ldots, \mathbb{A}'_m$ of L' to an inner radius of R_0 and an outer radius of $\tilde{R}_0$.
(4) Pick one of the outgoing curves, say C_i^+ of L. This curve is in general composed of several arcs, sitting on the outer circumference of L, running from one slit to the next. On one of the arcs we have the point P_i^+; subdivide this arc further by the radial line determind by P_i^+. We denote these arcs by $a_{i,1}, a_{i,2}, \ldots$, starting with the arc which begins at P_i^+, and numbered in the cyclic ordering given by C_i^+.
(5) Subdivide the annulus $\mathbb{A}'_i$ of L' into sectors $F'_{i,1}, F'_{i,2}, \ldots$ of anglular width proportiol to the arcs $a_{i,1}, a_{i,2}, \ldots$. It will not matter whether slits of L' lying on such radial cuts are put to the left or right side of the cut, as long as their (local) linear order is not effected.
(6) Insert each sector $F'_{i,k}$ into the annulus $\tilde{\mathbb{A}}_l$, such that its inner arc becomes the arc denoted by $a_{i,k}$.
(7) Rescale the annuli $\tilde{\mathbb{A}}_l$ to the have outer radius equal to 1.

The gluing process is depicted in the following figures.
The surface F in Figure [42] has $n = 2$, $m = 2$ and genus $g = 1$. The points $P_1^- = A$ and $P_2^- = B$ on the incoming boundary and points $P_1^+ = C$ and

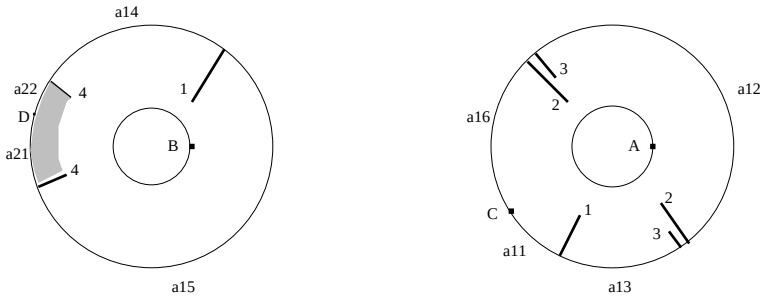

Figure 42: *The surface F of genus $g = 1$ and $n = 2$, $m = 2$, onto which another surface F' will be glued.*

$P_2^+ = D$ on the outgoing boundary are shown. The neighbourhood of the second outgoing curve C_2^+ is shaded as an emphasis.

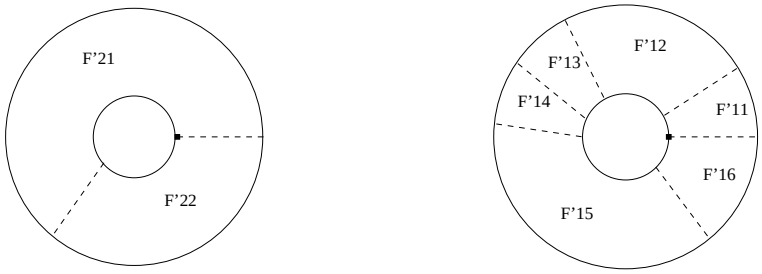

Figure 43: *The surface F' with $n' = 2$; there are no slits shown.*

This surface F' in Figure [43] will be glued to F, thus $n' = m = 2$. Note that – in order to keep the figures easy – we do not show any slits, and therefore the genus g' of F' and he number m' of outgoing bundary curves is not determined. The dashed lines cut F' into sectors $F'_{1,1}, \ldots, F'_{1,6}$ and $F'_{2,1}, F'_{2,2}$ according to the arcs $a_{1,1}, \ldots, a_{1,6}$ of the first outgoing curve C_1^+ of F, and the arcs $a_{2,1}, a_{2,2}$ of the second outgoing curve C_2^+ of F.
The last Figure [44] shows the composed surface; F is seen on the inner half of the two annuli, and the six sectors $F'_{1,1}, \ldots, F'_{1,6}$ from the first annulus of F' resp. the two sectors $F_{2,1}$ and $F_{2,2}$ of the second annulus of F' are inserted into the outer half of the two annuli.

The composition $\sharp$ makes the disjoint union $\mathfrak{M}^{\bullet\bullet} = \bigsqcup_{g,m,n} \mathfrak{M}_g^{\bullet\bullet}(m,n)$ of all moduli spaces into an H-space. It is strictly associative. If we had allowed

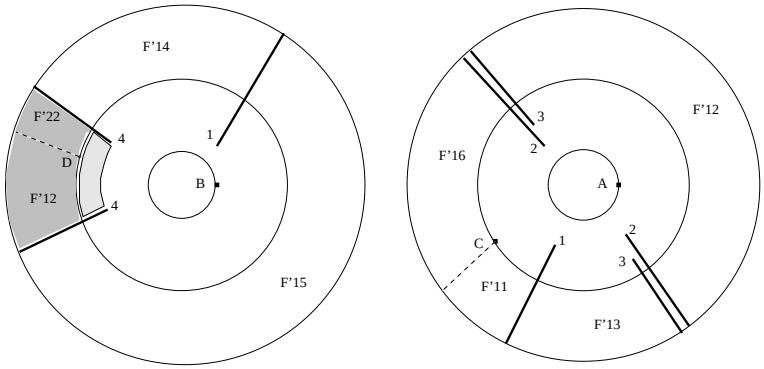

Figure 44: *The composition* $\tilde{F} = F' \sharp F$ *of both surfaces* F *and* F'.

disconnected surfaces in our moduli spaces, then the disjoint union of n resp.m cylinders would act as a left resp. right neutral element, but only up to homotopy. In other words, the sub-H-space given by $n = m = 1$ has a neutral element up to homotopy.

9.2 Properad and Operad Structure

With the compostion at hand we can now glue an arbitrary number of (connected) surfaces $F_1, \ldots, F_q$ with a total number of $m = m_1 + \ldots + m_q$ incoming curves to a single surface F with this number m of outgoing curves. Let $\underline{M} = (M_1, \ldots, M_q)$ an ordered decompositon of $[m] = \{1, \ldots, m\}$ into disjoint, non-empty subsets of cardinality $m_1, \ldots$ resp. m_q. Gluing the m_i incoming curves of F_i to those outgoing curves of F whose indices are in M_i defines a composition

$$\sharp_{\underline{M}} : N\mathfrak{M}^{\bullet\bullet}_{g_q}(m'_q, m_q) \times \ldots \times N\mathfrak{M}^{\bullet\bullet}_{g_1}(m'_1, m_1) \times N\mathfrak{M}^{\bullet\bullet}_{g}(m, n) \longrightarrow N\mathfrak{M}^{\bullet\bullet}_{g'+g}(m', n) \tag{9.5}$$

where $m = m_1 + \ldots + m_q$, $m' = m'_1 + \ldots + m'_q$, and $g' = g_q + \ldots + g_1$. Since these maps satisfy the desired associativity conditions, they turn the family of spaes $\mathfrak{M}^{\bullet\bullet}_g(m, n)$ into a properad. If we restrict to the subfamily $n = 1$, $m_1 = \ldots = m_q = 1$, we obtain an operad. This leads to a properad resp. operad structure on the homology of moduli spaces. In particular, one

can find an analogue of the Dyer-Lashof algebra acting on their mod 2-homology; see [B-2] for details in the case of parallel slit configurations.

References

[A] J. Abhau: *Die Homologie von Modulräumen Riemannscher Flächen - Berechnungen für $g \leq 2$.* Diplom thesis, Bonn (2005).

[ABE] J. Abhau, C.-F. Bödigheimer, R. Ehrenfried: *Homology computations for mapping class groups and moduli spaces of surfaces with boundary.* preprint (2005).

[Ab] W. Abikoff: *The Real Analytic Theory of Teichmüller Space.* Springer Verlag LNM vol. 820 (1976, 1989).

[B] J. Birman: *Braids, Links and Mapping Class Groups.* Annals of Math. Studies vol 82, Princeton University Press (1975).

[B-1] C.-F. Bödigheimer: *On the topology of moduli spaces, part I : Hilbert Uniformization.* Math.Gott. no. 7+8, SFB 170, Göttingen (1990).

[B-2] C.-F. Bödigheimer: *On the topology of moduli spaces, part II : Homology Operations.* Math.Gott. no. 9, SFB 170, Göttingen (1990).

[B-3] C.-F. Bödigheimer: *Interval exchange spaces and moduli spaces.* Contemp. Math. vol. 150, 33-50 (1993).

[B-4] C.-F. Bödigheimer: *Cyclic homology and moduli spaces of Riemann surfaces.* Asterisque 7 no. 226, 43-55 (1994).

[C] R. Courant: *Dirichlet's Principle, Conformal Mappings, and Minimal Surfaces.* Interscience Publishers (1950), Springer Verlag (1977).

[E] R. Ehrenfried: *Die Homologie der Modulräume berandeter Riemannscher Flächen von kleinem Geschlecht.* Ph.D. Thesis, Bonn University. Bonner Mathematische Schriften no. 306 (1997).

[F] O. Forster: *Riemannsche Flächen.* Springer Verlag (1977).

[GL] F.P. Gardiner, N. Lakic: *Quasiconformal Teichmüller Theory.* AMS Math. Surveys and Monographs vol. 76 (2000).

[H] D. Hilbert: *Zur Theorie der konformen Abbildung.* Nachr. Königl. Ges. Wiss. Göttingen, Math.-Phys. Klasse, (1909), 314-323.

[Z-1] M. Zaw: *The moduli space of non-classical directed Klein surfaces.* Ph.D. Thesis, Bonn University. Bonner Mathematische Schriften no. 313 (1998).

[Z-2] M. Zaw: *The homology groups of moduli spaces of Klein surfaces with one boundary curve.* Math. Proc. Cambridge Phil. Soc. 136 (2004), 599-615.

Mathematisches Institut
Universität Bonn
Beringstraße 1
D–53115 Bonn, Germany
email: boedigheimer@math.uni-bonn.de